Manuscript title

Chronic beta$_2$-adrenoceptor agonist treatment alters muscle proteome and functional adaptations induced by high intensity training in young men

Short title

Beta$_2$-adrenoceptor agonist alters adaptations to training

Morten Hostrup[1], Johan Onslev[1], Glenn Jacobson[2], Richard Wilson[3], Jens Bangsbo[1]

[1]Department of Nutrition, Exercise and Sports, University of Copenhagen, Copenhagen,

[2]Division of Pharmacy, School of Medicine, University of Tasmania, Hobart, Australia,

[3]Central Science Laboratory, University of Tasmania, Hobart, Australia

Corresponding Author
Morten Hostrup
Department of Nutrition, Exercise and Sports

University of Copenhagen

August Krogh 2nd floor

Universitetsparken 13

DK-2100 Copenhagen

Denmark
E-mail: mhostrup@nexs.ku.dk

Tel: +45 2447 4785
Fax: +45 3531 2179
ORCID ID: 0000-0002-6201-2483

This is an Accepted Article that has been peer-reviewed and approved for publication in the The Journal of Physiology, but has yet to undergo copy-editing and proof correction. Please cite this article as an 'Accepted Article'; doi: 10.1113/JP274970.

Keywords: physical activity, proteomics, metabolism, beta-agonists, adrenoceptors, adrenergic, VO2max, terbutaline, HIT, athletes

Word count: 7624

Figures (n=4) and tables (n=6)

Key Points

- While several studies have investigated the effects of exercise training in human skeletal muscle and the chronic effect of β_2-agonist treatment in rodent muscle, their effects on muscle proteome signature with related functional measures in humans are incomplete
- Herein we show that daily β_2-agonist treatment attenuates training-induced enhancements in exercise performance and maximal oxygen consumption, and alters muscle proteome signature and phenotype in trained young men
- Daily β_2-agonist treatment abolished several of the training-induced enhancements in muscle oxidative capacity and caused a repression of muscle metabolic pathways. Furthermore, β_2-agonist treatment induced a slow-to-fast twitch muscle phenotype transition
- The present study indicates that chronic β_2-agonist treatment confounds the positive effect of high intensity training on exercise performance and oxidative capacity, which is of interest for the large proportion of persons using inhaled β_2-agonists on a daily basis, including athletes

Abstract

Although the effects of training have been studied for decades, data on muscle proteome signature remodelling induced by high intensity training in relation to functional changes in humans remains incomplete. Likewise, β_2-agonists are frequently used to counteract exercise-induced bronchoconstriction, but the effects β_2-agonist treatment on muscle remodelling and adaptations to training are unknown. In a placebo-controlled parallel study, we randomized 21 trained men to four weeks of high intensity training with (HIT+β_2A) or without (HIT) daily inhalation of β_2-agonist (terbutaline, 4 mg/d). Of 486 proteins identified by mass-spectrometry proteomics of muscle biopsies sampled before and after the intervention, 32 and 85 were changing (FDR≤5%) with the intervention in HIT and HIT+β_2A. Proteome signature changes were different in HIT and HIT+β_2A (p=0.005), wherein β_2-agonist caused a repression of 25 proteins in HIT+β_2A compared to HIT, and an upregulation of 7 proteins compared to HIT. β_2-agonist repressed or even downregulated training-induced enrichment of pathways related to oxidative phosphorylation and glycogen metabolism, but upregulated pathways related to histone trimethylation and the nucleosome. Muscle contractile phenotype changed differently in HIT and HIT+β_2A (p≤0.001), with a fast-to-slow twitch transition in HIT and a slow-to-fast twitch transition in HIT+β_2A. β_2-agonist attenuated training-induced enhancements in maximal oxygen consumption (p≤0.01) and exercise performance (11.6 vs. 6.1%, p≤0.05) in HIT+β_2A compared to HIT. These findings indicate that daily β_2-agonist treatment attenuates the beneficial effects of high intensity training on exercise performance and oxidative capacity, and causes remodelling of muscle proteome signature towards a fast-twitch phenotype.

ABBREVIATIONS

ATP; adenosine triphosphate, β_2-agonist; beta$_2$-adrenoceptor agonist, cAMP; cyclic adenosine monophosphate, CSA; cross-sectional area, HIT; High intensity training + placebo group, HIT+β_2A; High intensity training + β_2-agonist group), MHC; myosin heavy chain, PKA; protein kinase A, TCA; tricarboxylic acid cycle, $\dot{V}o_{2max}$; maximal oxygen consumption.

Background

Exercise is essential for maintaining physical function and health, and is positively related to quality-of-life and life expectancy (Westerterp, 2001; Dhana *et al.* 2016). Thus, exercise is considered one of the best non-pharmacological strategies to prevent and even reverse several pathological conditions (Goodyear, 2008). In addition, exercise training is crucial for optimal performance in the vast majority of sport disciplines. High intensity training is widely practised because of its superior efficacy in improving physiological measures compared to low- and moderate intensity exercise (Milanovic *et al.* 2015). Only a few weeks of high intensity training improves cardiovascular fitness and induces several beneficial adaptations in skeletal muscle (Laursen & Jenkins, 2002; Hostrup & Bangsbo, 2017). The adaptations induced by high intensity training are related to major cellular perturbations in skeletal muscle that activate a variety of signalling pathways and gene programs (Arany *et al.* 2008; Canto *et al.* 2009; Powers *et al.* 2010; Hoffman *et al.* 2015; Brandt *et al.* 2016). However, while considerable progress has been made in understanding myocellular adaptations induced by training (Egan *et al.* 2011; Petriz *et al.* 2012; Hawley *et al.* 2014; Murton *et al.* 2014; Padrão *et al.* 2016; Powers *et al.* 2016; Sollanek *et al.* 2017), only few studies have investigated the effect of high intensity interval training on muscle proteome signature changes (Holloway *et al.* 2009; Egan *et al.* 2011; Hussey *et al.* 2012) and integrated such

changes with adaptations in muscle phenotype, contractile function and exercise performance in humans (Petriz *et al.* 2012; Padrão *et al.* 2016). Integrated approaches are needed to provide a global perspective on the relation between muscle remodelling and functional changes induced by training from a basic physiological standpoint and for future therapeutic applications.

A large proportion of the population experiences respiratory complications during physically demanding activities (Price *et al.* 2014). A common cause of this problem is asthma and exercise-induced bronchoconstriction with a prevalence of around 10% in Western countries (Cruz, 2007; Kainu *et al.* 2013). Inhaled β_2-adrenoceptor agonists (β_2-agonists) are used as first-line treatment of the bronchoconstriction associated with asthma and exercise-induced bronchoconstriction, and are as such among the most commonly prescribed medications worldwide (Rottenkolber *et al.* 2015). While the main application of inhaled β_2-agonists is to induce bronchodilation, a large proportion of the drug enters the systemic circulation and distributes to all organs (Jacobson *et al.* 2014; Dyreborg *et al.* 2016). The largest organ of the body, skeletal muscle, contains a high density of β_2-adrenoceptors (Williams *et al.* 1984; Jensen *et al.* 2002) that serve an important role in the adrenergic fight-or-flight response (Jensen *et al.* 2008; Emrick *et al.* 2010; Andersson *et al.* 2012; Hostrup *et al.* 2014a). Thus, acute inhalation of β_2-agonist has been shown to affect ion handling and energy production of skeletal muscle in trained young men (Hostrup *et al.* 2014a; Kalsen *et al.* 2016a; 2016b). Furthermore, when administered chronically, β_2-agonists induce hypertrophy and alter metabolic and contractile properties of skeletal muscle (Martineau *et al.* 1992; Dodd *et al.* 1996; Rajab *et al.* 2000; Hostrup *et al.* 2015). Therefore, β_2-agonists have been proposed as therapeutic agents to combat lifestyle-related diseases, muscle dysfunction and age-related

muscle atrophy (Lynch & Ryall, 2008; Joassard *et al.* 2013). However, despite their widespread use, it is unknown what effect daily inhalation of β_2-agonist has on training-induced adaptations in skeletal muscle and functional capacity in humans. This is important, since inhaled β_2-agonists are often used in conjunction with physical activity in persons with asthma and exercise-induced bronchoconstriction (Arie, 2012; Price *et al.* 2014). For instance, in some sports, as many as 50% of athletes use inhaled β_2-agonists in conjunction with training and competition (Parsons & Mastronarde, 2005). A better understanding of these β_2-agonist mediated effects on muscle proteome and phenotype could lead to improved treatment modalities in a diverse range of diseases such as muscle wasting and obesity.

Thus, the purpose of the present study was to investigate proteome signature and phenotype changes of skeletal muscle induced by high intensity training with and without concomitant daily treatment with β_2-agonist in therapeutic doses, integrating muscle remodeling with relevant functional measures related to maximal oxygen consumption ($\dot{V}O_{2max}$), exercise performance and muscle contractile properties in trained young men. We hypothesised that daily β_2-agonist treatment would alter training-induced modulation of muscle proteome signature and cause a shift towards a fast-twitch muscle phenotype.

Methods

Human subjects and ethics

Twenty-four healthy trained men were initially screened of which 21 were included in the study. Prior to inclusion, subjects received oral and written information about the aims and

contents of the study as well as possible risks involved, including side effects associated with the study drug (terbutaline). Each subject gave his oral and written informed consent. A physician screened each subject for unknown cardiopulmonary disease with lung and heart auscultation and electrocardiography. Inclusion criteria were males, aged 18 to 40 years, informed consent, a weekly training volume of 2-5 h and a body mass index between 19 and 25 kg/m^2. Exclusion criteria were smoking, allergy towards study drug, and chronic disease. Subjects were recreationally active, engaging in team sports, running, biking and/or light resistance training. Subjects were told to refrain from competitive events for the entire study and not to change their daily physical activities and nutritional habits, which were recorded. The study was conducted in accordance with the standards set by the 2013 version of the Declaration of Helsinki and was approved by the regional research ethics committee of Copenhagen, Denmark (H-4-2014-002). The study was registered in ClinicalTrials.gov (NCT02557581).

Study design

The study was designed as a block-randomized controlled parallel study with two groups: Either four weeks of high intensity training and daily inhalation of placebo (HIT, n = 9) or four weeks of high intensity training and daily inhalation of terbutaline (HIT+β_2A, n = 12). Upon inclusion, subjects were randomly allocated in the two groups, stratified for $\dot{V}O_{2max}$ and lean body mass. In HIT, subjects received a placebo inhalator (Turbohaler, AstraZeneca, Cambridge, UK) and in HIT+β_2A subjects received an inhalator of the selective β_2-agonist terbutaline (Bricanyl® Turbohaler 0.5 mg/dose, AstraZeneca, Cambridge, UK). Subjects were instructed to inhale eight doses once daily for 28 ± 1 days.

Study drugs

Terbutaline is a commonly prescribed short-acting β_2-agonist in Northern Europe, which has a high selectivity for the β_2-adrenoceptor (Baker, 2010) and a half-life of ~4 h (Krogh *et al.* 2017). The dosage of inhaled terbutaline administered (8×0.5 mg) in the present study is higher than that normally prescribed to asthmatics (Bricanyl® Turbohaler, product information, www.astrazeneca.com), but equivalent to the daily upper limit for inhaled salbutamol in competitive sports (2017 list of prohibited substances, www.wada-ama.org). The rationale for the dosage of 4 mg was to ensure an adequate systemic response, while staying within the current upper therapeutic limit in competitive sports. Systemic concentrations of terbutaline after inhalation of 4 mg have been shown to reach their peak within ½-1 h with concentrations of ~5-8 ng/mL (Dyreborg *et al.* 2016; Kreiberg *et al.* 2017). Such concentrations are equivalent or even higher than those observed after oral administration of 10 mg terbutaline (Elers *et al.* 2012; Dyreborg *et al.* 2016). To ensure a drug compliance of 100%, inhalations were monitored by study staff on a daily basis via online video tools (FaceTime/Skype). Because β_2-agonists may affect energy turnover and ion handling in skeletal muscle (Kalsen *et al.* 2014; Hostrup *et al.* 2014a; Hostrup *et al.* 2014b; Kalsen *et al.* 2016a), subjects inhaled their daily dose after exercise sessions at days of training. During non-training days, subjects inhaled their daily dose in the time frame of 9:00-18:00. The duration of treatment was based on a previous study showing that four weeks of treatment with terbutaline leads to adaptations in skeletal muscle of humans (Hostrup *et al.* 2015). Both subjects and investigators were blinded against treatment. Terbutaline Turbohalers were delivered by the regional pharmacy of Copenhagen, Denmark. Placebo Turbohalers were kindly delivered by AstraZeneca. Randomization was conducted in SPSS

(IBM, Armonk, NY, US) by staff that did not take part in any of the experimental procedures or data analysis.

Experimental protocol

Before the start of the intervention, subjects attended two trials at the laboratory separated by two days. At the first trial, subjects' thigh lean mass was determined by Dual-energy X-ray absorptiometry (DXA)(Lunar iDXA, GE Healthcase, Belgium). Subjects were placed in the scanner in supine position undressed. All DXA scans were performed with 10 min of supine rest before scanning to allow distribution of body fluids. To reduce intra-day variation, two scans were performed. After the scans, subjects rested in a supine position for 20 min and resting metabolic rate was determined by indirect calorimetry breath-by-breath with a gas analyzer system (Oxycon Pro, CareFusion, San Diego, CA, US) for 15 min. Subjects then performed a standardized warm-up on a bike ergometer at 100 W for 10 min (Monark LC4, Monark Exercise AB, Vansbro, Sweden). After warm-up, subjects' contractile properties of the quadriceps muscle were assessed by maximal voluntary contraction (MVC). After MVC, subjects' $\dot{V}O_{2max}$ and performance were determined during incremental cycling to exhaustion on the bike ergometer starting with 4 min of cycling at 100 W, in which substrate utilization was determined by indirect calorimetry as described by Jeukendrup & Wallis (2005), followed by 4 min at 150 W and 200 W, after which workload increased by 30 W every min until exhaustion.

At the second trial, thigh lean mass and resting metabolic rate were determined similar to the first trial to minimize day-to-day variation. Afterwards, subjects warmed up on the bike

ergometer for 4 min, followed by cycling at a workload corresponding to 60% of subjects' $\dot{V}O_{2max}$ for determination of substrate utilization at same relative intensity of $\dot{V}O_{2max}$. After the exercise, subjects' contractile properties of the quadriceps muscle were measured as performed during the first trial to minimize day-to-day variation. Subjects then rested for 30 min and had a muscle biopsy taken from the vastus lateralis of the right thigh using a Bergstrøm needle with suction (Bergstrøm, 1975). Prior to biopsy sampling, an incision (3 mm) was made through the skin and fascia at the vastus lateralis belly under local anesthesia (2 mL lidocaine without epinephrine, 20 mg/mL Xylocain®, AstraZeneca, Cambridge, UK).

After the second trial, subjects received either placebo or terbutaline according to their group.

Upon conclusion of the four-week intervention, subjects reported to two similar laboratory trials as the ones conducted before the intervention. To ensure complete washout of terbutaline (half-life ~4 h)(Krogh *et al.* 2017), post-testing was performed 2-3 days after last inhalation.

Subjects were told to abstain from caffeine, strenuous exercise and alcohol 48 h before each laboratory trial. To minimize variation, subjects ingested a standardized meal and fluid 1½ h before the laboratory trials.

Training intervention

During the four-week intervention, subjects performed a high intensity-training programme of 3 sessions pr. week on indoor spinning bikes. Each training session was supervised by an instructor and consisted of a standardised 10 min warm-up followed by three blocks of

exercise at ≈85% of maximum heart rate for 10 min with 30 s of all-out sprinting at the end of each 10 min block. Repeated all-out sprints of 30 s were chosen, as studies have shown that this type of training effectively induces adaptations in skeletal muscle (Hostrup & Bangsbo, 2017). During each training session, subjects wore heart rate monitors that fed subjects' heart rate to the instructor's iPad (iPad 4, Apple Inc., California, US) using Polar Team app (Polar Electro Denmark, Holte, Denmark), thus ensuring that subjects kept their target heart rate. Training adherence was 100% for all subjects, apart from one subject who missed one training session during the four-week intervention.

Experimental procedures

Contractile properties of the quadriceps muscle

Subjects' contractile properties of the quadriceps muscle were determined during MVC with percutaneous electrical muscle stimulation during and immediately after each contraction as described previously (Hostrup *et al.* 2015). Subjects were familiarized with two 3-4 s submaximal isometric muscle contraction at 40 and 70 % of MVC and with constant current electrostimulation, (Digitimer, model DS7AH, Welwyn garden city, England) at 100, 400, 700 and 999 mA with 400 V for 200 μs, before the first MVC. The electrostimulation used could activate 42.6 (± 3.3)% of subjects' peak MVC. Each MVC consisted of a 3-4 s maximal contraction with verbal encouragement. A potentiated twitch was applied when subjects reached their apparent peak MVC, as well as 1 s following relaxation. Peak twitch torque, time-to-peak twitch torque, half-relaxation time and voluntary activation level were calculated as previously described (Bachasson *et al.* 2013). Rate of force development was calculated as the average slope on the moment-time curve at the time interval 0-200 ms

relative to the onset of muscle contraction during MVC (Aagaard *et al.* 2002). Onset of muscle contraction was defined as the time point at which the moment curve increased to values above 2.5% of the magnitude of the moment achieved during MVC.

For each variable, a grand mean was calculated from the average of the two highest values from both trials. The distance from the base of patella to the middle of the Velcro strap on the ankle was registered and used to calculate torque in Newton meter (Nm).

Muscle biopsies

Sampled biopsies were divided in two pieces of which the first piece (20-30 mg) was mounted on an embedded medium (OCT Compound Tissue-Tek; Sakura Finetek, Zoeterwoude, The Netherlands), frozen in isopentane cooled to the freezing point in liquid nitrogen, and stored at -80°C until analysis for fiber type distribution, capillaries and fiber cross-sectional area by immunohistochemical analysis. The other biopsy piece (50-100 mg) was washed in ice-cold saline to reduce blood contamination, then dried and frozen in liquid nitrogen, and stored in cryo tubes for later proteomic, enzymatic and Western blot analyses. Prior to these analyses, each biopsy was freeze-dried and dissected free from apparent non-muscle tissue. The dissected muscle tissue was then divided in three pieces for proteomics (≈ 10 mg_{dw}), Western blotting (≈ 1.5 mg_{dw}) and enzyme activity assays (≈ 2 mg_{dw}). Because of inadequate muscle tissue yield from one subject in HIT, only proteomic analysis was performed for this subject.

Mass spectrometry proteomics

Proteins were extracted from muscle biopsies using two-step sequential extraction as described previously (Wilson *et al.* 2010; Nuez-Ortin *et al.* 2016; 2017). Proteins were extracted in progressively denaturing buffers (150 mM NaCl, 50 mM Tris, pH 8.0 followed by 7 M urea, 2 M thiourea, 50 mM Tris, pH 8.0), and 100 µg of protein sample was reduced using 10 mM DTT (overnight at 4 degrees), alkylated using 50 mM iodoacetamide (2 h at ambient temperature in the dark) then trypsin digested by co-precipitation. Briefly, 1 µg trypsin was spotted onto the wall of each sample Eppendorf tube then flushed into the sample with 1 mL 100% methanol chilled to -20 degrees. Samples were kept at -20 degrees overnight to allow co-precipitation of proteins with trypsin, then centrifuged in a benchtop microcentrifuge (5 min at 12,000×g) and pellets allowed to air-dry for 10 min. After addition of 100 mM ammonium bicarbonate, samples were then incubated for 5 h at 37 degrees with the further addition of 1 µg trypsin after 3 h. Samples were acidified by the addition of 1% formic acid and non-digested protein removed by centrifugation in a benchtop microcentrifuge (5 min at 12,000×g). Protein concentrations were estimated by Bradford assay (Bio-Rad) and 100 µg aliquots of each sample were cleaned up using ethanol precipitation (9:1 v/v ethanol:protein). Protein samples were trypsin digested at a ratio of 50:1 protein:trypsin using established methods (Wilson *et al.* 2010) and 1 µg aliquots of each peptide sample were analysed using an LTQ-Orbitrap and Ultimate 3000 nano RSLC system (Thermo Fisher Scientific, MA, USA) using published methods for separation and data-dependent acquisition (Wilson *et al.* 2016).

This method has been shown to be an effective approach to sample fractionation in complex and challenging tissues rich in structural proteins, such as cartilage (Wilson *et al.* 2010), whole fish larvae (Nuez-Ortin *et al.* 2016) and in white muscle (Nuez-Ortin *et al.* 2017) and

skeletal muscle (Barbé *et al.* 2017). Prior to processing the complete set of samples, a subset of six tissue biopsies was used to evaluate the extraction method for human skeletal muscle proteomics. Comparison of the extracted proteins indicated clear separation of the contractile proteins (e.g. actin, myosin and troponin) from readily soluble cytosolic proteins (e.g. glutathione S-transferases, 14-3-3 proteins and carbonic anhydrases) demonstrating the value of this approach to reduce sample complexity at the protein level.

Protein identification and data processing

Data files were imported into MaxQuant version 1.5.1.2 (http://maxquant.org/), where sequential extracts were defined as fractions of the same biological sample, and MS/MS spectra were searched against the Swiss-Prot Human reference proteome database (downloaded 18/03/2016; 20,1015 entries) using the Andromeda search engine. Default settings for protein identification by LTQ-Orbitrap MS/MS and label-free quantitation (LFQ) included a maximum of two missed cleavages, mass error tolerances of 20 ppm then 4.5 ppm for initial and main peptide searches, respectively, 0.5 Da tolerance for fragment ions, variable methionine oxidation and fixed cysteine carbamidomethylation. A false discovery rate of 1% was used for both peptide-spectrum matching and protein identification. The LFQ protein intensity values were extracted from the MaxQuant *proteinGroups.txt* file into Perseus software (http://perseus-framework.org/), filtered to remove proteins identified by reverse database matching and on the basis of modified peptides only and then log2-transformed. Proteins detected in fewer than twelve biological samples were also excluded and remaining missing values were imputed using low-abundance LFQ intensity values drawn from a normal distribution, according to default values in Perseus. In total, 9932 unique peptides were identified matching 783 proteins. Prior to statistical comparative

analysis, protein data were filtered for potential non-skeletal muscle contamination using the Human Protein Atlas (Uhlén *et al.* 2015; Thul *et al.* 2017). In accordance with the Human Protein Atlas (June 2017), 297 were determined not to be expressed at a protein level in skeletal muscle and were not included in further statistical analysis. The mass spectrometry proteomics data have been deposited to the ProteomeXchange Consortium via the PRIDE partner repository with the dataset identifier PXD005480.

Immunohistochemistry and confocal imaging

Muscle fiber type distribution, capillaries and fiber cross-sectional area were determined by immunohistochemistry and confocal imaging as described previously (Nyberg *et al.* 2016). Briefly, the embedded muscle samples were cut in transverse sections of 8 µm in a cryostat. Sections were fixed for 2 min in phosphate buffered saline (PBS, pH 7.2, Gibco 70013-016, Life Technologies Denmark, Nærum, Denmark) containing 2% formaldehyde and washed in a 1:10 wash buffer (Dako S3006, Glostrup, Denmark), and blocked for 10 min in PBS containing 1% BSA for immunohistochemical staining. Antibodies were diluted in antibody diluent (Dako S0809). First, capillaries and myofiber type IIA were visualized using biotinylated Ulex europaeus agglutinin I lectin (1:100; VECTB- 1065, VWR, Bie and Berntsen, Herlev, Denmark) and a monoclonal antibody (1:200; SC-71, Hybridoma Bank, Iowa City, IA), respectively. Second, myofiber borders were visualized using an antibody against laminin (1:500; Dako Z0097) together with myosin heavy chain (1:1000; Sigma-Aldrich Denmark M8421, Brøndby, Denmark) added for distinction of myofiber type I. Specific secondary antibodies [order listed: Streptavidin/FITC, (1:200; DAKO F0422), Alexa- 555 donkey anti-mouse (1:1000; Invitrogen A31570, Life Technologies Denmark), Alexa-350 goat anti-rabbit (1:1000; Invitrogen P10994) and Alexa-488 donkey anti-mouse

(1:1000; Invitrogen A21202)] were applied to each primary antibody. Three individual muscle fiber types were identified as type I (green), type IIA (red), and type IIX (unstained/black). Visualization was performed on a computer screen using a light microscope (Carl Zeiss, Germany), and all morphometric analysis were performed using a digital analysis program (ImageJ, NIH ImageJ). Two or more separate sections of a cross-section were used for analysis, and the cross-sectional area was assessed by manually drawing the perimeter around each selected section. The number of muscle fibers and capillaries within each section was counted, and capillary supply was subsequently expressed as capillaries per fiber (capillary-to-fibre ratio) and capillary density (cap/mm^2). Mean fiber area was assessed by manual drawing of the perimeter of each muscle fiber. All analyses were carried out manually by the same blinded investigator.

Immunoblotting and SDS page

Protein expression by Western blotting were determined as previously described (Thomassen *et al.* 2010). Protein concentration of each sample was determined with a BSA kit (ThermoFisher Scientific, MA, US). Samples were mixed with 6×Laemmli buffer (7 ml 0.5 M Tris-base, 3 ml glycerol, 0.93 g DTT, 1 g SDS and 1.2 mg bromophenol blue) and ddH_2O to reach equal protein concentration. Equal amount of protein was loaded in each well of pre-casted gels (Bio-Rad Laboratories, CA, US). Samples from each subject were loaded on the same gel with a mixed human muscle standard lysate loaded in two different wells used for normalization. Bands were visualised with ECL (Millipore, MA, US) and recorded with a digital camera (ChemiDoc MP Imaging System, Bio-Rad Laboratories, CA, US). Densitometry quantification of band intensity was done using Image Lab version 4.0 (Bio-Rad Laboratories, CA, US) and determined as the total band intensity adjusted for

background intensity. Primary antibodies used were citrate synthase (#ab96600, Abcam, MA, US), GLUT4 (#PA1-1065, ThermoFisher Scientific, MA, US), glycogen synthase (GS)(#3893, Cell Signalling Technology, MA, US), OXPHOS (#ab110411, Abcam, MA, US) and phosphofructokinase (Sc-166722, Santa Cruz Biotechnology, Inc, Dallas, US). The secondary antibodies used were HRP conjugated rabbit anti-sheep (P-0163), goat anti-mouse (P-0447, DAKO, Denmark) and goat anti-rabbit IgM/IgG (4010-05 Southern Biotech, AL, US).

Enzymatic activity

Maximal enzyme activity of citrate synthase, hexokinase, phosphofructokinase, and lactate dehydrogenase was quantified in muscle homogenates using fluorometric methods (Fluoroscan Ascent, Thermo Scientific, Waltham, MA) as described by Lowry & Passonneau (1972).

Statistics

Statistical analyses were performed in SPSS version 24. Sample size was based on previous studies of terbutaline (Hostrup *et al.* 2015; Dyreborg *et al.* 2016). Data were tested for normality using the Shapiro Wilks test and Q-Q plots. Data were normally distributed and magnitudes of outcome statistics are presented as means (± 95% confidence interval) and *p*-values to represent probability. To estimate within- and between-group changes with the intervention, two-tailed linear mixed modelling was used with group and trial included as fixed factors and a random factor for subjects for a full factorial design. Age was included as

a time-invariant covariate in the mixed model, since age has been shown to influence the response to β_2-agonists (White *et al.* 1994). For univariate correlation analyses, Pearson product-moment correlation coefficient was used. For the proteomic data, a series of mixed models were performed on the $\log_2$ expression for each protein to estimate protein-specific within- and between-group changes with the intervention. The false discovery rate (FDR) method as described by Storey & Tibshirani (2003) was used to control for multiple testing. Differently expressed proteins (FDR $\leq$ 5%) were subjected to functional annotation enrichment analysis (David Bioinformatics resources 6.8, NIH, US) based on gene ontology (GO) terms biological processes (GO:BP) and cellular components (GO:CC) as well as KEGG terms using an EASE score threshold of 0.1 and the Benjamini-Hochberg procedure to adjust p-values. Linear discriminant analysis-principal component analysis with varimax rotation was used to estimate between-group separation in the muscle proteome, only including the first eight principal components in the discriminant analysis because of the sample size of nine in HIT.

Results

Muscle proteome remodelling

Of the 486 proteins identified as human skeletal muscle proteins, training upregulated expression of 26 proteins (Table 2) and downregulated expression of 6 proteins (Table 3) in HIT (FDR $\leq$ 5%)(Fig. 1a), whereas concomitant daily inhalation of β_2-agonist upregulated expression of 34 proteins (Table 4) and downregulated expression of 51 proteins (Table 5) in HIT+β_2A (Fig. 1b). Inhalation of β_2-agonist caused a repression of 25 proteins in HIT+β_2A compared to HIT (group by trial interaction), and an upregulation of 7 proteins compared to

HIT (Table 6)(Fig. 1c). Proteome signature changes induced by the intervention in HIT and HIT+β_2A were markedly different as indicated by a clear separation of the two groups (Wilks' Lambda: 0.228, p = 0.005) in a principal component-discriminant analysis that explained 70% of total proteome variance (Fig. 1d).

Functional annotation enrichment analysis of differently expressed proteins (FDR ≤ 5%) based on gene ontology (GO) terms biological processes (GO:BP), cellular components (GO:CC) and KEGG pathways revealed different enrichments induced by the intervention in HIT and HIT+β_2A (Fig. 1e-g). In HIT, the most dominantly upregulated pathways were related to the mitochondria, in particular the oxidative phosphorylation, as well as metabolic pathways, including glycogen metabolism (Fig. 1e). In contrast, HIT+β_2A predominantly had an upregulation of pathways related to the cytosol, metabolism and cell-to-cell adhesion (Fig. 1f). HIT had a minor downregulation of pathways related to myosin filaments, protein kinases and the cytosol (Fig. 1e), whereas HIT+β_2A had several downregulated pathways, including those related to the cytosol and metabolism, including pyruvate and amino acid metabolism (Fig. 1f). Between-group analysis revealed that daily inhalation of β_2-agonist downregulated pathways related to glycogen metabolism and oxidative phosphorylation in HIT+β_2A compared to HIT, but upregulated pathways related to histone trimethylation and the nucleosome (Fig. 1g).

β_2-agonist blunts training-induced enhancements in $\dot{V}O_{2max}$ and exercise performance

A key observation was that inhalation of β_2-agonist completely blunted ($p \leq 0.01$) training-induced improvement in $\dot{V}O_{2max}$ and reduced ($p \leq 0.05$) enhancement in exercise

performance during incremental cycling to exhaustion (Fig. 2b). While training effectively augmented $\dot{V}O_{2max}$ in HIT ($p \leq 0.01$), HIT+β_2A had no relevant changes in $\dot{V}O_{2max}$ with the intervention (Fig. 2b). Furthermore, HIT had a two-fold greater enhancement in exercise performance compared to HIT+β_2A (11.6 vs. 6.1%, $p \leq 0.05$)(Fig. 2b). Between-group changes in $\dot{V}O_{2max}$ were still evident after adjusting for adaptations in resting metabolic rate and thigh lean mass (Fig. 2c), which indicates that the increase in $\dot{V}O_{2max}$ observed in HIT and the attenuating effect of β_2-agonist observed in HIT+β_2A were attributed to other factors than different adaptations in resting metabolic rate and hypertrophy of the exercising muscles. For training-induced enhancement in exercise performance, the between-group difference was also evident after adjusting for thigh lean mass (Fig. 2c). On the other hand, when adjusting for change in $\dot{V}O_{2max}$, no differences were observed in training-induced enhancement in exercise performance between the groups, thus indicating that the blunting effect of β_2-agonist on training-induced enhancement in performance in HIT+β_2A was related to the attenuating effect of β_2-agonist on improvement in $\dot{V}O_{2max}$.

Muscle capillary density has been shown to be related to $\dot{V}O_{2max}$ and associated with endurance performance (Saltin *et al.* 1977; Coyle *et al.* 1991). Nonetheless, we observed opposite adaptations in capillarisation of the vastus lateralis muscle considering that observed for $\dot{V}O_{2max}$ and exercise performance. Inhalation of β_2-agonist increased capillary density by 13% ($p \leq 0.05$) and capillary-to-fibre ratio by 21% ($p \leq 0.01$) in HIT+β_2A, whereas HIT had no relevant changes with the intervention (Fig. 2d). Thus, the increased $\dot{V}O_{2max}$ in HIT and blunted effect in HIT+β_2A might be related to an inhibitory effect of β_2-agonist on adaptations of the heart or mitochondrial oxidative capacity of the exercised muscles (Holloszy *et al.* 1984).

From proteomic analysis, we detected and grouped 13 proteins related to the tricarboxylic acid (TCA) cycle and 58 proteins related to oxidative phosphorylation of the mitochondria (Fig. 2a). For the TCA cycle, only minor changes were observed, in which succinate dehydrogenase flavoprotein subunit increased in both groups (Table 2+4), whereas aconitate hydratase and malate dehydrogenase decreased in HIT+β_2A (Table 5) with a between-group interaction for aconitate hydratase (Table 6). While proteomic analysis revealed no significant changes in citrate synthase, Western blotting showed a minor increase in HIT with a tendency towards a higher maximal enzymatic activity (Fig. 2f), but not statistically different from HIT+β_2A. There was a good correlation between the proteomic measurements of citrate synthase with that of Western blotting and enzymatic activity (Fig. 2g). In the oxidative phosphorylation, pronounced modulation was observed with the intervention. In HIT, abundance of a variety of the NADH dehydrogenase subcomplexes and ATP synthase subunits increased with the intervention (Table 2), whereas HIT+β_2A only had few significantly upregulated proteins (Table 4) and even blunted training-induced increase in abundance of four NADH dehydrogenase subcomplexes (Table 6). Consistent with this finding, Western blotting revealed an upregulation of overall abundance of OXPHOS complexes I-V in HIT ($p \leq 0.01$), whereas this effect was attenuated ($p \leq 0.01$) in HIT+β_2A (Fig. 2h).

β_2-agonist alters contractile phenotype

Some clearly distinct adaptations in muscle contractile properties and phenotype were observed between the groups. As shown in Fig. 3a+b, muscle proteome signature changed differently in HIT and HIT+β_2A as indicated by a between-group separation (Wilks' Lambda: 0.127, $p \leq 0.001$)(Fig. 3b) in a principal component-discriminant analysis that explained 80%

of the variance for the contractile proteins listed in Fig. 3a. These between-group differences were primarily driven by opposing adaptations in myosin light chains, troponin C and tropomyosin alpha and beta chains (Table 6), all of which may affect contractile properties and myofibrillar Ca^{2+} sensitivity (Greaser *et al.* 1988; Lamboley *et al.* 2014). Muscle fibre phenotype has historically been categorised according to MHC isoforms (Lutz *et al.* 1979; Harridge *et al.* 1996). Expression of myosin 1, the most highly expressed myosin isoform in type IIx fibres (Murgia *et al.* 2015), decreased with the intervention in HIT (log_2-fold change: -0.48, $p \leq 0.05$)(Fig. 3a+Table 2). Consistent with this observation, immunohistochemical analysis of the muscle biopsies revealed significant between-group changes ($p \leq 0.05$) with the intervention, in which HIT had a reduction in distribution of MHCIIx ($p \leq 0.05$)(Fig. 3c), whereas HIT+β_2A had an increase in distribution of MHCIIa by 4.1% ($p \leq 0.05$) (Fig. 3c). There was a high degree of consistency between myosin expression data determined by proteomics and MHC isoform distribution determined immunohistochemically (Fig. 3d). Aside from muscle contractile phenotype changes, HIT and HIT+β_2A had some different adaptations in sarcomere architecture and cell-to-cell adhesion. Compared to HIT, HIT+β_2A had an upregulation of actin- and anchoring related proteins actin and alpha-actinin-1 (Table 6).

Although a common effect of β_2-agonist treatment is muscle growth (Lynch & Ryall, 2008; Joassard *et al.* 2013; Hostrup *et al.* 2015), we observed a similar degree of thigh muscle hypertrophy in both groups with the intervention (Fig. 3f). At the muscle fibre level, however, histochemical analysis revealed that only HIT had an increase in mean cross-sectional area (CSA) of muscle fibres ($p \leq 0.05$), albeit not statistically different from HIT+β_2A (Fig. 3e). Despite the induced hypertrophy of the thigh, maximal isometric muscle

strength (peak torque) of the quadriceps did not change in either HIT or HIT+β_2A (Fig. 3g). In fact, when adjusting for adaptations in muscle fibre CSA, peak torque declined by 19% with the intervention in HIT ($p \leq 0.01$), whereas no change was observed in HIT+β_2A (Fig. 3g). Likewise, peak twitch torque declined by 17% ($p \leq 0.05$) and 27% ($p \leq 0.01$) in HIT when unadjusted and adjusted for muscle fibre CSA, respectively, whereas non-significant increases were observed in HIT+β_2A (Fig. 3h). Furthermore, muscle half-relaxation time was prolonged by 8 (± 6) ms with the intervention in HIT ($p \leq 0.05$), but not differently from HIT+β_2A that had no relevant change with the intervention (Fig. 3j). Degree of voluntary activation level (Fig. 3i), time-to-peak twitch torque (Fig. 3j) and rate of force development (Fig. 3k) of the quadriceps did not change in either group with the intervention.

β_2-agonist represses metabolic pathways

Various myocellular pathways regulate substrate choice during exercise, where glycogenolysis and glycolysis are predominant metabolic pathways for glucose metabolism and β-oxidation for lipid metabolism. Though only minor changes were observed in proteins related to lipid metabolism, HIT and HIT+β_2A had markedly diverse adaptations in the muscle proteome related to glycogenesis and glycogenolysis (Fig. 4a). Notably, in HIT+β_2A, inhalation of β_2-agonist attenuated the training-induced upregulation of glycogenin 1, glycogen debranching enzyme, glycogen synthase and glycogen phosphorylase observed in HIT (Table 6). HIT+β_2A even had a marked downregulation of glycogen debranching enzyme, glycogen phosphorylase and glycogenin 1 (Fig. 4a, Table 5). Likewise, glycogen synthase, the rate-limiting enzyme in glycogenesis, which was the most significantly upregulated protein of the proteome in HIT (Fig. 4a, Table 2), did not change in HIT+β_2A. For further confirmation of this observation, Western blotting of glycogen synthase revealed

a 25% increase in glycogen synthase abundance in HIT ($p \leq 0.01$), which was blunted ($p \leq 0.01$) in HIT+β_2A (Fig. 4d). In the glycolytic pathway, some minor changes were observed. Abundance of hexokinase 1 increased with the intervention in HIT+β_2A compared to HIT (Table 4 and 6) with a concurrent minor repression of lactate dehydrogenase A chain (Table 5). Partly in accordance with these observations, enzymatic analysis showed that maximal activity of hexokinase increased ($p \leq 0.01$)(Fig. 4b) and lactate dehydrogenase decreased in HIT+β_2A ($p \leq 0.05$)(Fig. 4c). In contrast, HIT had a minor increase in abundance and maximal activity of the glycolytic rate-limiting enzyme, phosphofructokinase ($p \leq 0.05$)(Fig. 4b+d), and a marked increase in lactate dehydrogenase activity ($p \leq 0.01$)(Fig. 4c). In general, principal component analysis revealed a good association between the different assays used to determine changes in glycogen synthase, hexokinase, phosphofructokinase and lactate dehydrogenase (Fig. 4f).

The major sources of substrate for ATP production during endurance exercise are glucose and free fatty acids, whereas the contribution of amino acids is negligible (Jeukendrup & Wallis, 2005). As a measure for changes in substrate choice during exercise, we determined subjects' glucose and fat oxidation by indirect calorimetry during steady state cycling both at same absolute intensity at 100 W and at an intensity corresponding to 60% of $\dot{V}O_{2max}$ before and after the intervention. While HIT had an increase in the relative contribution of glucose oxidation by 15.9 (± 7.0) percentage-points and a corresponding decline in fat oxidation with the intervention at both intensities ($p \leq 0.01$), concomitant daily inhalation of β_2-agonist blunted ($p \leq 0.05$) this training-induced change in substrate choice in HIT+β_2A (Fig. 4g).

Discussion

Herein we have described adaptations in skeletal muscle proteome signature and phenotype induced by high intensity training with and without concomitant daily inhalation of β_2-agonist, as well as associated physiological adaptations in exercise performance, $\dot{V}O_{2max}$, muscle contractile properties and substrate utilization during exercise. The most important findings were that daily β_2-agonist treatment altered training-induced changes in muscle proteome signature and phenotype and attenuated enhancements in $\dot{V}O_{2max}$ and exercise performance.

While several studies have investigated the effect of high intensity interval training in human skeletal muscle (Laursen & Jenkens, 2002; Padrão *et al.* 2016; Hostrup & Bangsbo, 2017) and the chronic effect of β_2-agonist treatment in rodent muscle (Pearen *et al.* 2009; Koopman *et al.* 2010), the present study is first to describe changes in muscle proteome signature and phenotype with related functional measures after an intervention with high intensity interval training and β_2-agonist treatment in humans. Consistent with previous studies (Laursen & Jenkins, 2002; Milanovic *et al.* 2015), we observed that high intensity interval training effectively enhanced $\dot{V}O_{2max}$ and exercise performance in trained young men. More surprisingly, however, we observed that daily inhalation of β_2-agonist, terbutaline, completely blunted training-induced increase in $\dot{V}O_{2max}$ and reduced enhancement in exercise performance. Although few studies in rodents have shown that systemic chronic treatment with β_2-agonist clenbuterol blunts the effect of endurance training on exercise capacity (Ingalls *et al.* 1996; Duncan *et al.* 2000), the present study is first to show such effect of β_2-agonists in humans. Furthermore, the present study is first to show that daily β_2-agonist

treatment attenuates the enhancing effect of endurance training on $\dot{V}O_{2max}$. It is noteworthy that inhalation of β_2-agonist, in close to therapeutic doses, is capable of blunting the enhancing effects of high intensity interval training on $\dot{V}O_{2max}$ and exercise performance. This is possibly related to the relatively high systemic bioavailability of inhaled β_2-agonists (Dyreborg *et al.* 2016), partitioning into muscle (Jacobson *et al.* 2014) and inducing a continuous adrenergic fight-or-flight response (Emrick *et al.* 2010; Andersson *et al.* 2012; Hostrup *et al.* 2014a). Accordingly, high inhalation of terbutaline has been shown to induce significant β_2-adrenergic stimulation of skeletal muscle in humans (Hostrup *et al.* 2014a; Kalsen *et al.* 2016a; 2016b). The dosage of inhaled terbutaline (4 mg) administered in the present has also been shown to result in systemic concentrations that exceed those observed after oral administration of 10 mg terbutaline (Elers *et al.* 2012; Dyreborg *et al.* 2016).

Our observations indicate that the attenuating effect of β_2-agonist on training-induced enhancement in exercise performance and $\dot{V}O_{2max}$, at least in part, may be related to remodelling of muscle proteome signature and phenotype. Indeed, enhancements in exercise performance and $\dot{V}O_{2max}$ observed in HIT were complemented by pronuonced upregulation of mitochondrial proteins and metabolic pathways in skeletal muscle, in particular related to oxidative phosphorylation and glycogen metabolism, being consistent with reports in humans and rodents (Holloway *et al.* 2009; Egan *et al.* 2011; Sollanek *et al.* 2017). In contrast, however, we observed that daily inhalation of β_2-agonist attenuated training-induced upregulation of NADH dehydrogenase subcomplexes of the oxidative phosphorylation and even caused a repression of carbohydrate metabolic pathways, including downregulation of glycogen debranching enzyme, glycogen phosphorylase and glycogenin 1. The repressing effect of β_2-agonist treatment on oxidative capacity and carbohydrate metabolism is in

agreement with observations in rodents (Torgan *et al.* 1995), in which chronic β_2-agonist treatment has been shown to compromise mitochondrial function and pyruvate oxidation capacity (Hoshino *et al.* 2012). Given that a high capacity for oxidative metabolism and glycogenolysis is essential for energy and ion homeostasis of skeletal muscle and thus performance during intense exercise (Allen *et al.* 2008; Ørtenblad *et al.* 2013; Hostrup & Bangsbo, 2017), the attenuating effect of β_2-agonist on training-induced upregulation of oxidative and glycogenolytic proteins may explain why training-induced enhancement in exercise performance was reduced in HIT+β_2A. Furthermore, it may be speculated that β_2-agonist treatment compromised glycogen storage in HIT+β_2A compared to HIT in the present study, since glycogenin 1 was repressed by β_2-agonist treatment and that training-induced upregulation of glycogen synthase was blunted in HIT+β_2A. Accordingly, expression and activity of glycogenin are proportional to glycogen content in human skeletal muscle (Shearer *et al.* 2000; Shearer *et al.* 2005) and glycogen synthase is a key enzyme in muscle glycogenesis (Bouskila *et al.* 2010). Thus, future studies should elucidate whether β_2-agonist-induced proteome changes in glycogen metabolism are associated with alterations in resting glycogen content and rate of glycogenolysis during exercise.

Aside from the effect of β_2-agonist treatment on training-induced adaptations in oxidative and metabolic pathways, we observed that terbutaline also modulated adaptations in muscle contractile phenotype and function. While the high intensity interval training regime undertaken induced a shift in muscle contractile phenotype from type IIx towards type IIa, concomitant daily inhalation of β_2-agonist induced a muscle phenotype transition from slow- towards a fast-twitch phenotype. Although slow-to-fast-twitch muscle phenotype transition is a common phenomenon after chronic β_2-agonist treatment in rodents (Dodd *et al.* 1996;

Zhang *et al.* 1996; Jones *et al.* 2004; Sirvent *et al.* 2014), this has not been described previously in humans. The contractile slow-to-fast twitch phenotype changes induced by chronic β_2-agonist treatment have been shown to be associated with enhancements in maximal force and acceleration of relaxation time of skeletal muscle in both rodents and humans (Martineau *et al.* 1992; Dodd *et al.* 1996; Zhang *et al.* 1996; Hostrup *et al.* 2015; 2016). On the contrary to these findings, however, β_2-agonist treatment did not increase muscle force and peak twitch force or accelerate relaxation time of the quadriceps in HIT+β_2A. This discrepancy is possibly related to the fact that β_2-agonist treatment did not induce muscle hypertrophy or changes in expression of sarcoplasmic reticulum Ca^{2+} ATPase (SERCA) isoforms compared to placebo in the present study. As such, muscle hypertrophy has been shown to be the main mechanism by which chronic β_2-agonist treatment enhances peak twitch and tetanic muscle force (Dodd *et al.* 1996; Hostrup *et al.* 2015). Furthermore, studies suggest that the accelerating effect of chronic β_2-agonist treatment on muscle relaxation time is attributed to upregulation of SERCAI (Zhang *et al.* 1996; Hostrup *et al.* 2015) and concurrent downregulation of SERCAII and SERCA-regulatory subunit phospholamban (Zhang *et al.* 1996). In HIT, on the other hand, peak twitch force declined and relaxation time prolonged with the intervention, thus indicating that changes in contractile phenotype were associated with some of the adaptations in quadriceps contractile properties. Given that muscle contractile properties are highly dependent on muscle fibre contractile phenotype (Harridge *et al.* 1996), the phenotype changes in HIT and HIT+β_2A may explain why HIT had a slower muscle relaxation time and a decline in peak twitch torque after the intervention.

The observation that β_2-agonist treatment alters training-induced remodelling of proteome signature and phenotype in relation to oxidative capacity as well as metabolic and contractile properties of skeletal muscle coincides with the acute and temporal changes in gene transcription profile observed in rodent skeletal muscle upon β_2-adrenergic stimulation (Spurlock *et al.* 2006; Pearen *et al.* 2009). Acute β_2-adrenoceptor activation has profound effects on global gene expression in rodent skeletal muscle, where β_2-agonists formoterol and clenbuterol have been shown to enrich a variety of pathways, including those related to metabolism, cell-to-cell communication and transcriptional regulation (Spurlock *et al.* 2006; Pearen *et al.* 2009). Apart from the proteome adaptations in metabolism, we also observed that β_2-agonist treatment induced an upregulation proteome pathways related to transcriptional regulation compared to training alone, including histone trimethylation and the nucleosome. Because β_2-adrenergic stimulation induces an adrenergic fight-or-flight response in skeletal muscle (Emrick *et al.* 2010; Andersson *et al.* 2012), nucleosome adaptations to chronic β_2-agonist treatment seem to be a logical consequence of the continuous adrenergic myocellular stress and signalling (Pearen *et al.* 2009). Indeed, non-selective β-agonist isoproterenol has been shown to induce expression of histones in cells (Lim & Juhnn, 2016), and Spurlock *et al.* (2006) observed that chronic β_2-agonist treatment with clenbuterol upregulated transcriptional and translational initiator genes in rodent muscle. In addition, we observed that β_2-agonist treatment upregulated proteome pathways related to adherens junction, cell-to-cell communication and cytoskeleton, inducing expression of actin and alpha-actinin 1 compared to training alone. It could be speculated that such upregulations may have impacted between-fibre force transfer positively in HIT+β_2A (Nelson *et al.* 2016; Hughes *et al.* 2016; Lambert *et al.* 2016). Thus, a potential modulation of sarcomere architecture and cell-to-cell adhesion induced by β_2-agonist treatment may explain why

HIT+β_2A had no reduction in peak twitch torque and mass-specific peak torque compared to HIT.

While the acute and chronic response to β_2-adrenoceptor activation may have some similarities with exercise training (Spurlock *et al.* 2006; Pearen *et al.* 2009; Hostrup *et al.* 2015), the present study, as well as studies in rodents (Ingalls *et al.* 1996; Lynch *et al.* 1996; Duncan *et al.* 2000; Mounier *et al.* 2007), indicate that chronic β_2-agonist treatment confounds the effect of exercise training. For instance, although a common feature of chronic β_2-agonist treatment is muscle hypertrophy in rodents and humans (Lynch & Ryall, 2008; Joassard *et al.* 2013; Hostrup *et al.* 2015), we observed no apparent induction of hypertrophy by β_2-agonist treatment compared to training alone. This observation is consistent with observations in rodents, in which exercise training blunts or reduces the hypertrophic effect chronic clenbuterol treatment (Duncan *et al.* 2000; Mounier *et al.* 2007). The mechanisms underlying the attenuating effect of endurance training on the hypertrophic response to β_2-agonist treatment remain to be elucidated, but may be related to the fact that endurance training interferes with the growth-promoting signalling (Coffey & Hawley, 2017) induced upon β_2-adrenergic stimulation (Koopman *et al.* 2010).

In summary, the present study showed that daily inhalation of β_2-agonist alters adaptations to four weeks of high intensity endurance training in recreationally active young men, both in terms of proteome signature remodelling and phenotype changes of skeletal muscle, but also in relation to functional adaptations in exercise performance, $\dot{V}O_{2max}$, muscle contractile properties and substrate utilization during exercise. The most notably observation was that β_2-

agonist treatment attenuated training-induced enhancements in exercise performance and $\dot{V}O_{2max}$, as well as blunted adaptations in oxidative phosphorylation and glycogen metabolism of skeletal muscle. Furthermore, that β_2-agonist treatment induced a slow-to-fast twitch muscle fibre type transition. Future studies should elucidate the molecular mechanisms underlying the confounding effect of β_2-agonist treatment on adaptations to endurance training.

Acknowledgements

We express our gratitude to the technical assistance of Anders Krogh Lemminger, Anders Schulze Gad, Christian Narkowicz, Jens Jung Nielsen, Martin Thomassen, Nanna Krogh, Peter Piil and Søren Jessen throughout the study in the collection, analyses, and interpretation of data.

Translational Perspective (word count: 249/250)

This study tested the hypothesis that daily inhalation of β_2-agonist alters adaptations in muscle proteome signature incurred from high intensity training. We observed that β_2-agonist terbutaline blunted training-induced upregulation of proteome pathways related to oxidative phosphorylation and glycogen metabolism, while concurrently inducing a slow-to-fast twitch muscle phenotype transition. Notably, terbutaline also attenuated training-induced enhancements in $\dot{V}O_{2max}$ and exercise performance. These findings are of interest for the large proportion of persons using inhaled β_2-agonists on a daily basis, including athletes, and indicate that athletes who have a high use of β_2-agonist may benefit from lessening their

reliance on β_2-agonist inhalers. This is also consistent with clinical guidelines, where regular reliance on β_2-agonist is indicative of poor asthma control. Furthermore, the present study provides a fingerprint of some of the muscle proteome and phenotype changes induced by high intensity training with and without β_2-agonist treatment, which may be used for future therapeutic applications. Indeed, it has long been proposed that β_2-agonists have a therapeutic potential in treatment of muscle atrophic conditions (Lynch & Ryall, 2008; Joassard *et al.* 2013), despite their potential cardiomyotoxic effects when administered in high doses. Accordingly, chronic β_2-agonist treatment may repress oxidative capacity (Léger *et al.* 2011) and induce collagen infiltration and necrosis in rodent cardiac muscle (Duncan *et al.* 2000; Burniston *et al.* 2002; 2005; 2006; Gregorevic *et al.* 2005). Thus, the attenuating effect of daily β_2-agonist treatment on training-induced enhancements in exercise performance and $\dot{V}O_{2max}$ may involve modulating effects in both skeletal and cardiac muscle.

References

Aagaard P, Simonsen EB, Andersen JL, Magnusson P & Dyhre-Poulsen P (2002). Increased rate of force development and neural drive of human skeletal muscle following resistance training. *J Appl Physiol* **93**, 1318-1326.

Allen DG, Lamb GD & Westerblad H (2008). Skeletal muscle fatigue: cellular mechanisms. *Physiol Rev* **88**: 287-332.

Andersson DC, Betzenhauser MJ, Reiken S, Umanskaya A, Shiomi T & Marks AR (2012). Stress-induced increase in skeletal muscle force requires protein kinase A phosphorylation of the ryanodine receptor. J Physiol 590, 6381-6387.

Arany Z, Foo SY, Ma Y, Ruas JL, Bommi-Reddy A, Girnun G, Cooper M, Laznik D, Chinsomboon J, Rangwala SM, Baek KH, Rosenzweig A & Spiegelman BM (2008). HIF-independent regulation of VEGF and angiogenesis by the transcriptional coactivator PGC-1alpha. *Nature* **451**, 1008-1012.

Arie S (2012). What can we learn from asthma in elite athletes? *BMJ* **344**, e2556.

Bachasson D, Millet GY, Decorte N, Wuyam B, Levy P & Verges S (2013). Bachasson, D. *et al*. Quadriceps function assessment using an incremental test and magnetic neurostimulation: a reliability study. *J Electromyogr Kinesiol* **23**, 649-658.

Baker JG (2010). The selectivity of beta-adrenoceptor agonists at human beta1-, beta2- and beta3-adrenoceptors. *Br J Pharmacol* **160**, 1048-1061.

Barbé C, Bray F, Gueugneau M, Devassine S, Lause P, Tokarski C, Rolando C & Thissen JP (2017). Comparative Proteomic and Transcriptomic Analysis of Follistatin-Induced Skeletal Muscle Hypertrophy. *J Proteome Res*. doi: 10.1021/acs.jproteome.7b00069. [Epub ahead of print]

Bergstrøm J (1975) .Percutaneous needle biopsy of skeletal muscle in physiological and clinical research. *Scand J Clin Lab Invest* **35**, 609-616.

Bouskila M, Hunter RW, Ibrahim AF, Delattre L, Peggie M, van Diepen JA, Voshol PJ, Jensen J & Sakamoto K (2010). Allosteric regulation of glycogen synthase controls glycogen synthesis in muscle. *Cell Metab* **12**, 456-466.

Brandt N, Gunnarsson TP, Hostrup M, Tybirk J, Nybo L, Pilegaard H & Bangsbo J (2016). Impact of adrenaline and metabolic stress on exercise-induced intracellular signaling and

PGC-1α mRNA response in human skeletal muscle. *Physiol Rep* **4**, pii: e12844. doi: 10.14814/phy2.12844.

Burniston JG, Ng Y, Clark WA, Colyer J, Tan LB & Goldspink DF (2002). Myotoxic effects of clenbuterol in the rat heart and soleus muscle. *J Appl Physiol* **93**, 1824-1832.

Burniston JG, Chester N, Clark WA, Tan LB & Goldspink DF (2005). Dose-dependent apoptotic and necrotic myocyte death induced by the beta2-adrenergic receptor agonist, clenbuterol. *Muscle Nerve* **32**, 767-774.

Burniston JG, Clark WA, Tan LB & Goldspink DF (2006). Dose-dependent separation of the hypertrophic and myotoxic effects of the beta(2)-adrenergic receptor agonist clenbuterol in rat striated muscles. *Muscle Nerve* **33**, 655-663.

Cantó C, Gerhart-Hines Z, Feige JN, Lagouge M, Noriega L, Milne JC, Elliott PJ, Puigserver P & Auwerx J (2009). AMPK regulates energy expenditure by modulating NAD+ metabolism and SIRT1 activity. *Nature* **458**, 1056-1060.

Coffey VG & Hawley JA (2017). Concurrent exercise training: do opposites distract? *J Physiol* **595**, 2883-2896.

Coyle EF, Feltner ME, Kautz SA, Hamilton MT, Montain SJ, Baylor AM, Abraham LD & Petrek GW (1991). Physiological and biomechanical factors associated with elite endurance cycling performance. *Med Sci Sports Exerc* **23**, 93-107.

Cruz AA (2007). Global surveillance, *prevention and control of chronic respiratory diseases: a comprehensive approach. Editors: Bousquet, J, Khaltaev, NG. World Health Organization.*

Dhana K, Koolhaas CM, Berghout MA, Peeters A, Ikram MA, Tiemeier H, Hofman A, Nusselder W & Franco OH (2016). Physical activity types and life expectancy with and without cardiovascular disease: the Rotterdam Study. *J Public Health*. [Epub ahead of print]

Dodd SL, Powers SK, Vrabas IS, Criswell D, Stetson S & Hussain R (1996). Effects of clenbuterol on contractile and biochemical properties of skeletal muscle. *Med Sci Sports Exerc* **28**, 669-676.

Duncan ND, Williams DA & Lynch GS (2000). Deleterious effects of chronic clenbuterol treatment on endurance and sprint exercise performance in rats. *Clin Sci (Lond)* **98**, 339-347.

Dyreborg A, Krogh N, Backer V, Rzeppa S, Hemmersbach P & Hostrup M (2016). Pharmacokinetics of Oral and Inhaled Terbutaline after Exercise in Trained Men. *Front Pharmacol* **7**, 150. doi: 10.3389/fphar.2016.00150.

Egan B, Dowling P, O'Connor PL, Henry M, Meleady P, Zierath JR & O'Gorman DJ (2011). 2-D DIGE analysis of the mitochondrial proteome from human skeletal muscle reveals time course-dependent remodelling in response to 14 consecutive days of endurance exercise training. *Proteomics* **11**, 1413-1428.

Elers J, Hostrup M, Pedersen L, Henninge J, Hemmersbach P, Dalhoff K & Backer V (2012). Urine and serum concentrations of inhaled and oral terbutaline. *Int J Sports Med* **33**, 1026-1033.

Emrick MA, Sadilek M, Konoki K & Catterall WA (2010). Beta-adrenergic-regulated phosphorylation of the skeletal muscle Ca(V)1.1 channel in the fight-or-flight response. *Proc Natl Acad Sci* **107**, 18712-18717.

Goodyear LJ (2008). The exercise pill--too good to be true? *N Engl J Med* **359,** 1842-1844.

Greaser ML, Moss RL & Reiser PJ (1988). Variations in contractile properties of rabbit single muscle fibres in relation to troponin T isoforms and myosin light chains. *J Physiol* **406**, 85-98.

Gregorevic P, Ryall JG, Plant DR, Sillence MN & Lynch GS (2005). Chronic beta-agonist administration affects cardiac function of adult but not old rats, independent of beta-adrenoceptor density. *Am J Physiol Heart Circ Physiol* **289**, 344-349.

Harridge SD, Bottinelli R, Canepari M, Pellegrino MA, Reggiani C, Esbjörnsson M & Saltin B (1996). Whole-muscle and single-fibre contractile properties and myosin heavy chain isoforms in humans. *Pflugers Arch* **432**, 913-920.

Hawley JA, Hargreaves M, Joyner MJ & Zierath JR (2014). Integrative biology of exercise. *Cell* **159**, 738-749.

Hoffman NJ, Parker BL, Chaudhuri R, Fisher-Wellman KH, Kleinert M, Humphrey SJ, Yang P, Holliday M, Trefely S, Fazakerley DJ, Stöckli J, Burchfield JG, Jensen TE, Jothi R, Kiens B, Wojtaszewski JF, Richter EA & James DE (2015). Global Phosphoproteomic Analysis of Human Skeletal Muscle Reveals a Network of Exercise-Regulated Kinases and AMPK Substrates. *Cell Metab* **22**, 922-935.

Holloszy JO & Coyle EF (1984). Adaptations of skeletal muscle to endurance exercise and their metabolic consequences. *J Appl Physiol Respir Environ Exerc Physiol* **56**, 831-838.

Holloway KV, O'Gorman M, Woods P, Morton JP, Evans L, Cable NT, Goldspink DF & Burniston JG (2009). Proteomic investigation of changes in human vastus lateralis muscle in response to interval-exercise training. *Proteomics* **9**, 5155-5574.

Hoshino D, Yoshida Y, Holloway GP, Lally J, Hatta H & Bonen A (2012). Clenbuterol, a β2-adrenergic agonist, reciprocally alters PGC-1 alpha and RIP140 and reduces fatty acid and pyruvate oxidation in rat skeletal muscle. *Am J Physiol Regul Integr Comp Physiol* **302**, 373-384.

Hostrup M & Bangsbo J (2017). Limitations in intense exercise performance of athletes - effect of speed endurance training on ion handling and fatigue development. *J Physiol* **595**, 2897-2913.

Hostrup M, Kalsen A, Onslev J, Jessen S, Haase C, Habib S, Ørtenblad N, Backer V & Bangsbo J (2015). Mechanisms underlying enhancements in muscle force and power output during maximal cycle ergometer exercise induced by chronic β2-adrenergic stimulation in men. *J Appl Physiol* **119**, 475-486.

Hostrup M, Kalsen A, Ortenblad N, Juel C, Mørch K, Rzeppa S, Karlsson S, Backer V & Bangsbo J (2014a). β2-adrenergic stimulation enhances Ca2+ release and contractile properties of skeletal muscles, and counteracts exercise-induced reductions in Na+-K+-ATPase Vmax in trained men. *J Physiol* **592**, 5445-5459.

Hostrup M, Kalsen A, Bangsbo J, Hemmersbach P, Karlsson S & Backer V (2014b). High-dose inhaled terbutaline increases muscle strength and enhances maximal sprint performance in trained men. *Eur J Appl Physiol* **114**, 2499-2508.

Hostrup M, Kalsen A, Auchenberg M, Bangsbo J & Backer V (2016). Effects of acute and 2-week administration of oral salbutamol on exercise performance and muscle strength in athletes. *Scand J Med Sci Sports* **26**, 8-16.

Hughes DC, Marcotte GR, Marshall AG, West DWD, Baehr LM, Wallace MA, Saleh PM, Bodine SC & Baar K (2016). Age-related Differences in Dystrophin: Impact on Force Transfer Proteins, Membrane Integrity, and Neuromuscular Junction Stability. J *Gerontol A Biol Sci Med Sci*, pii: glw109 [Epub ahead of print]

Hussey SE, Sharoff CG, Garnham A, Yi Z, Bowen BP, Mandarino LJ & Hargreaves M (2013). Effect of exercise on the skeletal muscle proteome in patients with type 2 diabetes. *Med Sci Sports Exerc* **45**, 1069-1076.

Højlund K, Yi Z, Hwang H, Bowen B, Lefort N, Flynn CR, Langlais P, Weintraub ST & Mandarino LJ (2008). Characterization of the human skeletal muscle proteome by one-dimensional gel electrophoresis and HPLC-ESI-MS/MS. *Mol Cell Proteomics* **7**, 257-267.

Ingalls CP, Barnes WS & Smith SB (1996). Interaction between clenbuterol and run training: effects on exercise performance and MLC isoform content. *J Appl Physiol* **80**, 795-801.

Jacobson GA, Yee KC, Premilovac D & Rattigan S (2014). Enantioselective disposition of (R/S)-albuterol in skeletal and cardiac muscle. *Drug Test Anal* **6**, 563-567.

Jensen J, Brennesvik EO, Bergersen H, Oseland H, Jebens E & Brørs O (2002). Quantitative determination of cell surface beta-adrenoceptors in different rat skeletal muscles. *Pflugers Arch* **444**, 213-219.

Jensen J, Grønning-Wang LM, Jebens E, Whitehead JP, Zorec R & Shepherd PR (2008). Adrenaline potentiates insulin-stimulated PKB activation in the rat fast-twitch epitrochlearis muscle without affecting IRS-1-associated PI 3-kinase activity. *Pflugers Arch* **456**, 969-978.

Jeukendrup AE & Wallis GA (2005). Measurement of substrate oxidation during exercise by means of gas exchange measurements. *Int J Sports Med* **26**, 28-37.

Joassard OR, Durieux AC & Freyssenet DG (2013). β2-Adrenergic agonists and the treatment of skeletal muscle wasting disorders. *Int J Biochem Cell Biol* **45**, 2309-2321.

Jones SW, Baker DJ, Gardiner SM, Bennett T, Timmons JA & Greenhaff PL (2004). The effect of the beta2-adrenoceptor agonist prodrug BRL-47672 on cardiovascular function, skeletal muscle myosin heavy chain, and MyoD expression in the rat. J Pharmacol Exp Ther 311, 1225-1131.

Kainu A, Pallasaho P, Piirilä P, Lindqvist A, Sovijärvi A & Pietinalho A (2013). Increase in prevalence of physician-diagnosed asthma in Helsinki during the Finnish Asthma Programme: improved recognition of asthma in primary care? A cross-sectional cohort study. *Prim Care Respir J* **22**, 64-71.

Kalsen A, Hostrup M, Karlsson S, Hemmersbach P, Bangsbo J & Backer V (2014). Effect of inhaled terbutaline on substrate utilization and 300-kcal time trial performance. *J Appl Physiol* **117**, 1180-1187.

Kalsen A, Hostrup M, Söderlund K, Karlsson S, Backer V & Bangsbo J (2016a). Inhaled Beta2-Agonist Increases Power Output and Glycolysis during Sprinting in Men. *Med Sci Sports Exerc* **48**, 39-48.

Kalsen A, Hostrup M, Backer V & Bangsbo J (2016b). Effect of formoterol, a long-acting β2-adrenergic agonist, on muscle strength and power output, metabolism, and fatigue during maximal sprinting in men. *Am J Physiol Regul Integr Comp Physiol* **310**, 1312-1321.

Koopman R, Gehrig SM, Léger B, Trieu J, Walrand S, Murphy KT & Lynch GS (2010). Cellular mechanisms underlying temporal changes in skeletal muscle protein synthesis and

breakdown during chronic {beta}-adrenoceptor stimulation in mice. *J Physiol* **588**, 4811-4823.

Kreiberg M, Becker V, Jessen S, Rzeppa S, Hemmersbach P, Backer V & Hostrup M (2017). Influence of exercise in normal and hot ambient conditions on the pharmacokinetics of inhaled terbutaline in trained men. *Scand J Med Sci Sports* **27**, 692-703.

Krogh N, Rzeppa S, Dyreborg A, Dehnes Y, Hemmersbach P, Backer V & Hostrup M (2017). Terbutaline Accumulates in Blood and Urine following Daily Therapeutic Inhalation. *Med Sci Sports Exerc*, doi: 10.1249/MSS.0000000000001199. [Epub ahead of print]

Lambert M, Richard E, Duban-Deweer S, Krzewinski F, Deracinois B, Dupont E, Bastide B & Cieniewski-Bernard C (2016). O-GlcNAcylation is a key modulator of skeletal muscle sarcomeric morphometry associated to modulation of protein-protein interactions. *Biochim Biophys Acta* **1860**, 2017-2030.

Lamboley CR, Murphy RM, McKenna MJ & Lamb GD (2014). Sarcoplasmic reticulum Ca2+ uptake and leak properties, and SERCA isoform expression, in type I and type II fibres of human skeletal muscle. *J Physiol* **592**, 1381-1395.

Laursen PB & Jenkins DG (2002). The scientific basis for high-intensity interval training: optimising training programmes and maximising performance in highly trained endurance athletes. *Sports Med* **32**, 53-73.

Léger B, Koopman R, Walrand S, Gehrig SM, Murphy KT & Lynch GS (2011). Chronic formoterol administration reduces cardiac mitochondrial protein synthesis and oxidative capacity in mice. *Int J Cardiol* **146**, 270-272.

Lim JA & Juhnn YS (2016). Isoproterenol increases histone deacetylase 6 expression and cell migration by inhibiting ERK signaling via PKA and Epac pathways in human lung cancer cells. *Exp Mol Med* **48**, e204.

Lowry OH & Passonneau JV (1972). A Flexible System of Enzymatic Analysis. *New York: Academic,* 237–249.

Lutz H, Weber H, Billeter R & Jenny E (1979). Fast and slow myosin within single skeletal muscle fibres of adult rabbits. *Nature* **281**, 142-144.

Lynch GS & Ryall JG (2008). Role of beta-adrenoceptor signaling in skeletal muscle: implications for muscle wasting and disease. *Physiol Rev* **88**, 729-767.

Lynch GS, Hayes A, Campbell SP & Williams DA (1996). Effects of beta 2-agonist administration and exercise on contractile activation of skeletal muscle fibers. *J Appl Physiol* **81**, 1610-1618.

Martineau L, Horan MA, Rothwell NJ & Little RA (1992). Salbutamol, a beta 2-adrenoceptor agonist, increases skeletal muscle strength in young men. *Clin Sci (Lond)* **83**, 615-621.

Milanović Z, Sporiš G & Weston M (2015). Effectiveness of High-Intensity Interval Training (HIT) and Continuous Endurance Training for VO2max Improvements: A Systematic Review and Meta-Analysis of Controlled Trials. *Sports Med* **45**, 1469-1481.

Mounier R, Cavalié H, Lac G & Clottes E (2007). Molecular impact of clenbuterol and isometric strength training on rat EDL muscles. *Pflugers Arch* **453**, 497-507.

Murgia M, Nagaraj N, Deshmukh AS, Zeiler M, Cancellara P, Moretti I, Reggiani C, Schiaffino S & Mann M (2015). Single muscle fiber proteomics reveals unexpected mitochondrial specialization. *EMBO Rep* **16**, 387-395.

Murton AJ, Billeter R, Stephens FB, Des Etages SG, Graber F, Hill RJ, Marimuthu K & Greenhaff PL (2014). Transient transcriptional events in human skeletal muscle at the outset of concentric resistance exercise training. *J Appl Physiol* **116**, 113-125.

Nelson CE *et al*. (2016). In vivo genome editing improves muscle function in a mouse model of Duchenne muscular dystrophy. *Science* **351**, 403-407.

Nuez-Ortin WG, Carter CG, Nichols PD & Wilson R (2016). Sequential protein extraction as an efficient method for improved proteome coverage in larvae of Atlantic salmon (Salmo salar). *Proteomics* **16**, 2043-2047.

Nuez-Ortín WG, Carter CG, Wilson R, Cooke IR, Amoroso G, Cobcroft JM & Nichols PD (2017). Triploid Atlantic salmon shows similar performance, fatty acid composition and proteome response to diploids during early freshwater rearing. *Comp Biochem Physiol Part D Genomics Proteomics* **22**, 67-77.

Nyberg M, Fiorenza M, Lund A, Christensen M, Rømer T, Piil P, Hostrup M, Christensen PM, Holbek S, Ravnholt T, Gunnarsson TP & Bangsbo J (2016). Adaptations to Speed Endurance Training in Highly Trained Soccer Players. *Med Sci Sports Exerc* **48**, 1355-1364.

Padrão AI, Ferreira R, Amado F, Vitorino R & Duarte JA (2016). Uncovering the exercise-related proteome signature in skeletal muscle. *Proteomics* **16**, 816-830.

Parsons JP & Mastronarde JG (2005). Exercise-induced bronchoconstriction in athletes. *Chest* **128**, 3966-3974.

Pearen MA, Ryall JG, Lynch GS & Muscat GE (2009). Expression profiling of skeletal muscle following acute and chronic beta2-adrenergic stimulation: implications for hypertrophy, metabolism and circadian rhythm. *BMC Genomics* **10**, 448.

Petriz BA, Gomes CP, Rocha LA, Rezende TM & Franco OL (2012). Proteomics applied to exercise physiology: a cutting-edge technology. *J Cell Physiol* **227**, 885-898.

Powers SK, Duarte J, Kavazis AN & Talbert EE (2010). Reactive oxygen species are signalling molecules for skeletal muscle adaptation. *Exp Physiol* **95**, 1-9.

Powers SK, Radak Z & Ji LL (2016). Exercise-induced oxidative stress: past, present and future. *J Physiol* **594**, 5081-5092.

Price OJ, Hull JH, Backer V, Hostrup M & Ansley L (2014). The impact of exercise-induced bronchoconstriction on athletic performance: a systematic review. *Sports Med* **44**, 1749-1761.

Rajab P, Fox J, Riaz S, Tomlinson D, Ball D & Greenhaff PL (2000). Skeletal muscle myosin heavy chain isoforms and energy metabolism after clenbuterol treatment in the rat. *Am J Physiol Regul Integr Comp Physiol* **279**, 1076-1081.

Rottenkolber M, Voogd E, van Dijk L, Primatesta P, Becker C, Schlienger R, de Groot MC, Alvarez Y, Durand J, Slattery J, Afonso A, Requena G, Gil M, Alvarez A, Hesse U, Gerlach R, Hasford J, Fischer R, Klungel OH & Schmiedl S (2015). Time trends of period prevalence rates of patients with inhaled long-acting beta-2-agonists-containing prescriptions: a European comparative database study. *PLoS One* **10**, e0117628.

Saltin B, Henriksson J, Nygaard E, Andersen P & Jansson E (1977). Fiber types and metabolic potentials of skeletal muscles in sedentary man and endurance runners. *Ann N Y Acad Sci* **301**, 3-29.

Schertzer JD, Plant DR, Ryall JG, Beitzel F, Stupka N & Lynch GS (2005). Beta2-agonist administration increases sarcoplasmic reticulum Ca2+-ATPase activity in aged rat skeletal muscle. *Am J Physiol Endocrinol Metab* **288**, 526-533.

Shearer J, Marchand I, Sathasivam P, Tarnopolsky MA & Graham TE (2000). Glycogenin activity in human skeletal muscle is proportional to muscle glycogen concentration. *Am J Physiol Endocrinol Metab* **278**, 177-180.

Shearer J, Wilson RJ, Battram DS, Richter EA, Robinson DL, Bakovic M & Graham TE (2005). Increases in glycogenin and glycogenin mRNA accompany glycogen resynthesis in human skeletal muscle. *Am J Physiol Endocrinol Metab* **289**, 508-514.

Sirvent P, Douillard A, Galbes O, Ramonatxo C, Py G, Candau R & Lacampagne A (2014). Effects of chronic administration of clenbuterol on contractile properties and calcium homeostasis in rat extensor digitorum longus muscle. *PLoS One* **9**, e100281. doi: 10.1371/journal.pone.0100281. eCollection 2014.

Sollanek KJ, Burniston JG, Kavazis AN, Morton AB, Wiggs MP, Ahn B, Smuder AJ & Powers SK (2017). Global Proteome Changes in the Rat Diaphragm Induced by Endurance Exercise Training. *PLoS One* **12**, e0171007. doi: 10.1371/journal.pone.0171007. eCollection 2017.

Spurlock DM, McDaneld TG & McIntyre LM (2006). Changes in skeletal muscle gene expression following clenbuterol administration. *BMC Genomics* **7**, 320.

Storey JD & Tibshirani R (2003). Statistical significance for genomewide studies. *Proc Natl Acad Sci* **100**, 9440-9445.

Thomassen M, Christensen PM, Gunnarsson TP, Nybo L & Bangsbo J (2010). Effect of 2-wk intensified training and inactivity on muscle Na+-K+ pump expression, phospholemman (FXYD1) phosphorylation, and performance in soccer players. *J Appl Physiol* **108**, 898-905.

Thul PJ et al. (2017). A subcellular map of the human proteome. *Science* **356**. pii: eaal3321. doi: 10.1126/science.aal3321. Epub 2017 May 11.

Torgan CE, Etgen GJ Jr, Kang HY & Ivy JL (1995). Fiber type-specific effects of clenbuterol and exercise training on insulin-resistant muscle. *J Appl Physiol* **79**, 163-167.

Uhlén M. *et al* (2015). Proteomics. Tissue-based map of the human proteome. *Science* **347**, 1260419.

Westerterp KR (2001). Pattern and intensity of physical activity. *Nature* **410**, 539.

White M, Roden R, Minobe W, Khan MF, Larrabee P, Wollmering M, Port JD, Anderson F, Campbell D, Feldman AM & Bristow MR (1994). Age-related changes in beta-adrenergic neuroeffector systems in the human heart. *Circulation* **90**, 1225-1238.

Williams RS, Caron MG & Daniel K (1984). Skeletal muscle beta-adrenergic receptors: variations due to fiber type and training. *Am J Physiol* **246**, 160-167.

Wilson R, Diseberg AF, Gordon L, Zivkovic S, Tatarczuch L, Mackie EJ, Gorman JJ & Bateman JF (2010). Comprehensive profiling of cartilage extracellular matrix formation and maturation using sequential extraction and label-free quantitative proteomics. *Mol Cell Proteomics* **9**, 1296-1313.

Wilson R, Golub SB, Rowley L, Angelucci C, Karpievitch YV, Bateman JF & Fosang AJ (2016). Novel elements of the chondrocyte stress response identified using an in vitro model of mouse cartilage degradation. *J Proteome Res*, doi:10.1021/acs.jproteome.5b01115.

Zhang KM, Hu P, Wang SW, Feher JJ, Wright LD, Wechsler AS, Spratt JA & Briggs FN (1996). Salbutamol changes the molecular and mechanical properties of canine skeletal muscle. *J Physiol* **496**, 211-220.

Ørtenblad N, Westerblad H & Nielsen J (2013). Muscle glycogen stores and fatigue. *J Physiol* **591**, 4405-4413.

Competing interests

Authors have no competing interests.

Author contributions

Morten Hostrup designed the study, participated in data collection, analysis and interpretation, and drafted the manuscript. Johan Onslev conducted the human experiments and participated in data analysis and interpretation, as well as in drafting of the manuscript. Glenn A. Jacobson and Richard Wilson conducted the muscle proteomic analysis and assisted in the bioinformatics analysis and interpretation, as well as in revising the manuscript. Jens Bangsbo participated in designing the study and in the analysis and interpretation data, as well as in drafting of the manuscript. All authors approved the final version of the manuscript.

Additional information

The mass spectrometry proteomics data have been deposited to the ProteomeXchange Consortium via the PRIDE partner repository with the dataset identifier PXD005480.

Funding

The study was supported by a grant from the Danish Ministry of Culture and Team Denmark.

Figure legends

Fig. 1. Effect of four weeks of high intensity training with (HIT+β_2A, n = 12) and without (HIT, n = 9) daily inhalation of terbutaline (4 mg/d) on proteome signature of the vastus lateralis muscle in trained men. **a-c**: Volcano plots of within-group changes in skeletal muscle proteins (486 proteins) in HIT (**a**) and HIT+β_2A (**b**) as well as between-group interaction (HIT+β_2A – HIT) (**c**). Green scale indicates %-false discovery rate (FDR). **d**: Gaussian fit of frequency distribution of discriminant canonical function score of within-group changes in proteome signature using principal component-discriminant analysis (PCA-DA) of the eight first principal components that explained 70% of total proteome variance. **e-g**: Enrichment analysis of the 10 most up- (blue) and downregulated (red) pathways (GO: biological processes, GO: cellular component, and KEGG pathways) in HIT (**e**) and HIT+β_2A (**f**) as well as between-group (HIT+β_2A – HIT) (**g**).

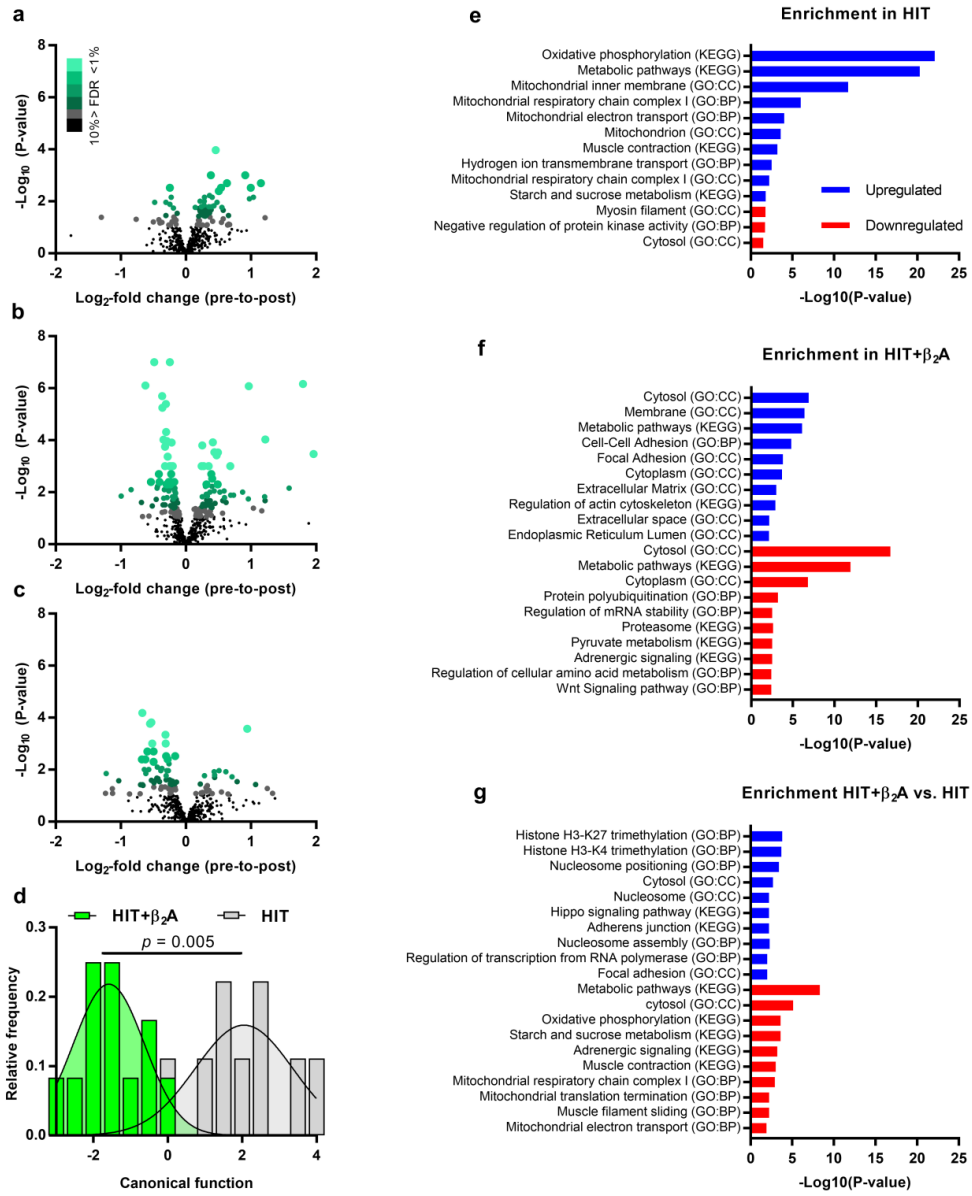

Fig. 2. Effect of four weeks of high intensity training with (HIT+β_2A, n = 12) and without (HIT, n = 9) daily inhalation of terbutaline (4 mg/d) on outcomes related to exercise performance and oxidative capacity in trained men. **a**: Heat map of mean Z-score changes of the proteome related to tricarboxylate acid cycle and oxidative phosphorylation in HIT and HIT+β_2A as well as between-group interaction (HIT+β_2A − HIT). **b**: Mean (± 95%CI) maximal oxygen consumption ($\dot{V}O_{2max}$)(left y-axis) and incremental peak power output (iPPO)(right y-axis). **c**: Mean (± 95%CI) relative change in $\dot{V}O_{2max}$ and iPPO when unadjusted and adjusted for thigh lean mass (TLM). **d**: Mean (± 95%CI) capillary density (left y-axis) and capillary-to-fiber ratio (right y-axis). **e**: Representative image of immunohistochemical analysis; myosin heavy chain I (red), IIa (green/brown), IIx (black), laminin (blue), capillary (light green). **f**: Mean (± 95%CI) expression (left y-axis) and maximal activity (right y-axis) of citrate synthase (CS). **g**: Bivariate correlation between intensity (log_2-expression) of CS as determined by proteomics (y-axis) versus expression (left y-axis) and maximal activity (right y-axis) of CS as determined by Western blotting and fluorometrically, respectively. **h**: Mean (± 95%CI) relative change in abundance of OXPHOS complex I-V (CI-V) determined by Western blotting. **i**: Representative blots of CS and OXPHOS CI-V. $^{\#}$Between-group interaction ($p \leq 0.05$). $^{\#\#}$Between-group interaction ($p \leq 0.01$). *Within-group difference from pre ($p \leq 0.05$). **Within-group difference from pre ($p \leq 0.01$).

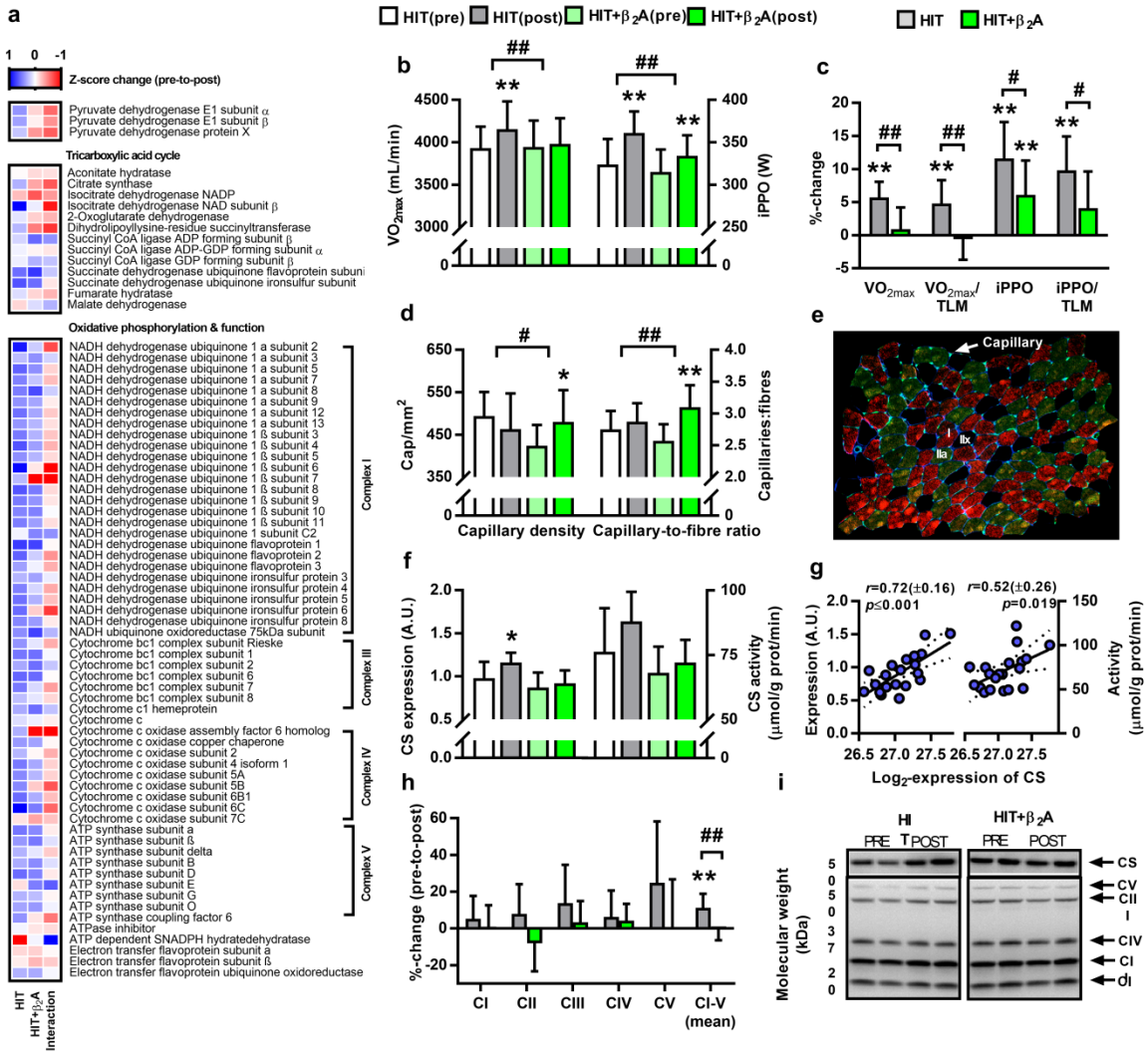

Fig. 3. Effect of four weeks of high intensity training with (HIT+β_2A, n = 12) and without (HIT, n = 9) daily inhalation of terbutaline (4 mg/d) on outcomes related to contractile phenotype and function in trained men. **a**: Heat map of mean Z-score changes of the proteome related to the cytoskeleton and contractile phenotype in HIT and HIT+β_2A as well as between-group interaction (HIT+β_2A − HIT). **b**: Gaussian fit of frequency distribution of discriminant canonical function score of within-group changes in the proteins listed in (**a**) using a principal component-discriminant analysis (PCA-DA) of the eight first principal components that explained 80% of the variance. **c**: Mean (± 95%CI) change in myosin heavy

chain (MHC) isoform distribution. **d**: PCA of intensity (log_2-expression) of myosin isoforms determined by proteomics (white circles) and MHC isoform distribution determined immunohistochemically (purple circles). **e-k**: Mean (± 95%CI) values for muscle mass and contractile properties. CSA: cross-sectional area. #Between-group interaction ($p \leq 0.05$). ##Between-group interaction ($p \leq 0.01$). *Within-group difference from pre ($p \leq 0.05$). **Within-group difference from pre ($p \leq 0.01$).

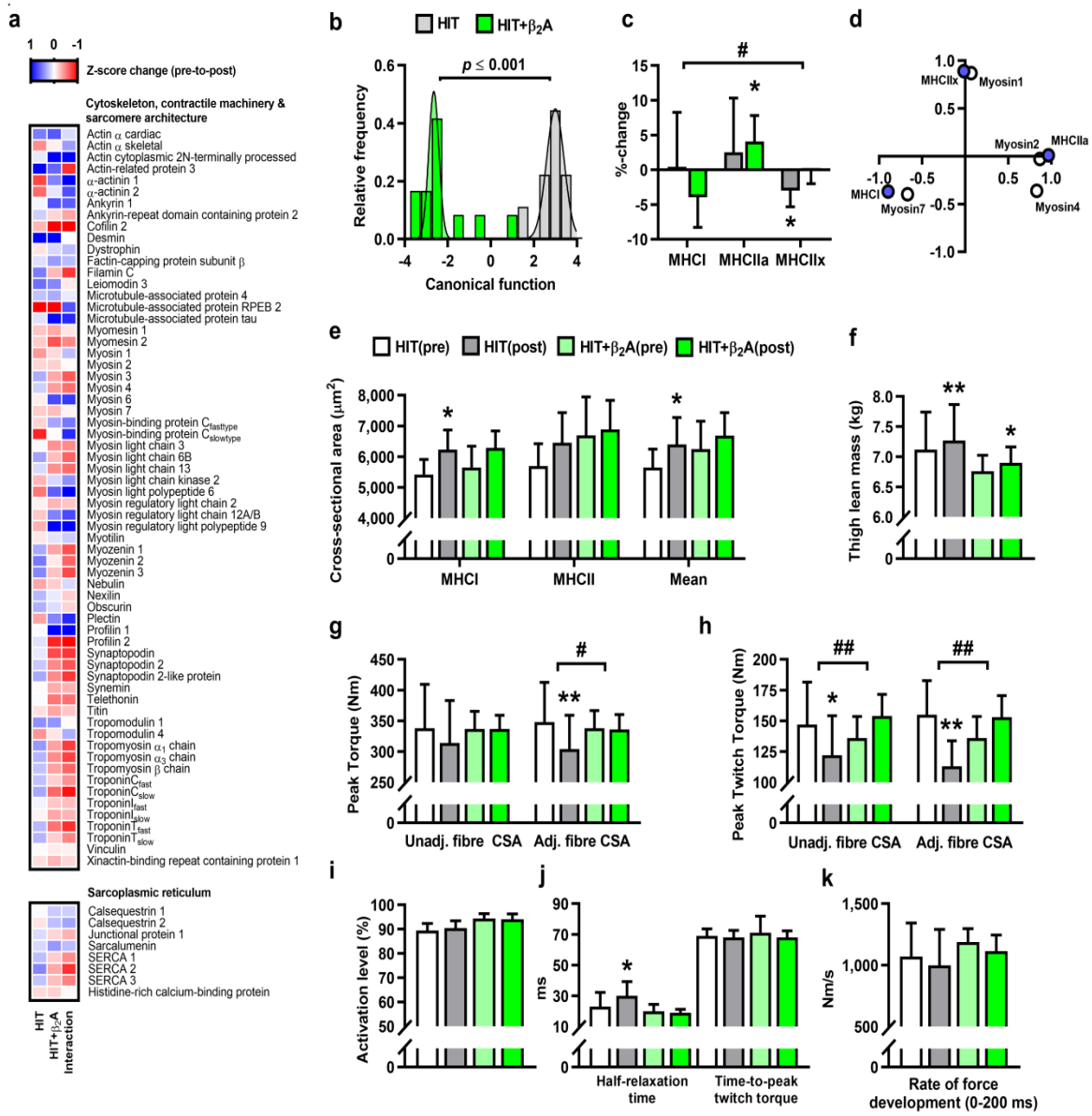

Fig. 4. Effect of four weeks of high intensity training with (HIT+β_2A, n = 12) and without (HIT, n = 9) daily inhalation of terbutaline (4 mg/d) on outcomes related to metabolism in trained men. **a**: Heat map of mean Z-score changes of the proteome related to glycogenesis, glycogenolysis, glycolysis and lipid metabolism with the intervention in HIT and HIT+β_2A as well as between-group interaction (HIT+β_2A − HIT). **b-c**: Mean (± 95%CI) maximal activity for hexokinase (HK), phosphofructokinase (PFK) and lactate dehydrogenase (LDH). **d**: Mean (± 95%CI) relative change in abundance of GLUT4, glycogen synthase (GS) and PFK determined by Western blotting. **e**: Representative blots of GLUT4, GS and PFK. **f**: Principal component analysis of intensity (log_2-expression) of GS, HK, LDHA, LDHB and PFK determined by proteomics (white circles), GS and PFK expression determined by Western blotting (yellow circles), and HK, LDH and PFK activity determined fluorumetrically (purple circles). **g**: Mean (± 95%CI) relative contribution of carbohydrate (COX)(red bars) and fat oxidation (FOX)(black bars) during cycling at 60% of maximal oxygen consumption ($\dot{V}O_{2max}$) (left side) and at 100 W (right side). #Between-group interaction ($p \leq 0.05$). ##Between-group interaction ($p \leq 0.01$). *Within-group difference from pre ($p \leq 0.05$). **Within-group difference from pre ($p \leq 0.01$).

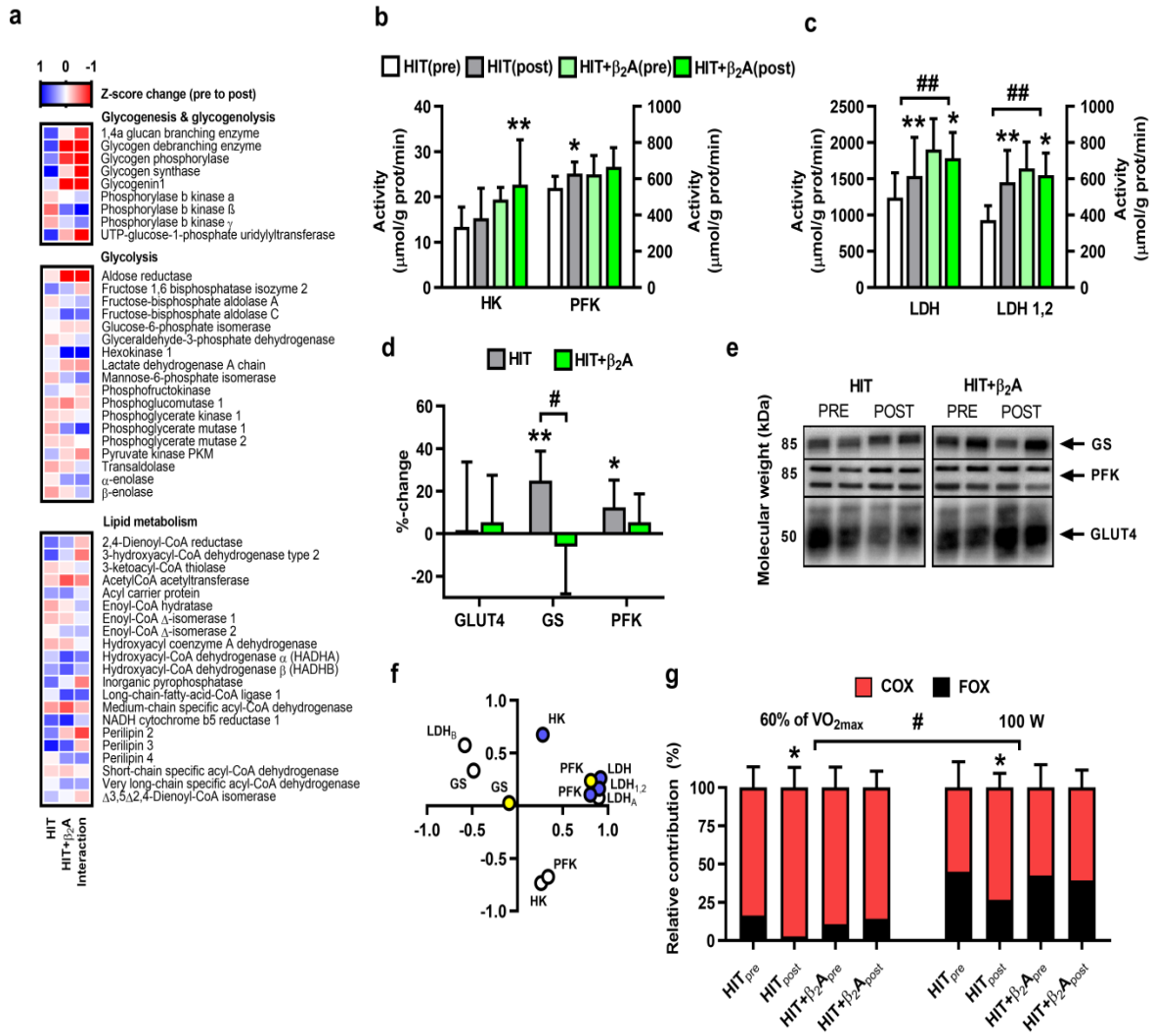

Tables

Table 1. Subject characteristics

	HIT (n = 9)	HIT+β_2A (n = 12)	Between-group difference (*p*-value)
Age (years)	24.7 (± 3.0)	23.5 (± 1.7)	0.47
Height (cm)	184 (± 3)	185 (± 2)	0.85
Weight (kg)	78.4 (± 6.7)	77.6 (± 5.5)	0.86
Lean body mass (kg)	61.5 (± 4.4)	60.6 (± 2.9)	0.72
$\dot{V}O_{2max}$ (mL/min)	3932 (± 233)	3945 (± 329)	0.95
MHCI (%)	49.4 (± 9.6)	49.2 (± 6.8)	0.97
MHCIIa (%)	44.2 (± 9.4)	45.8 (± 5.9)	0.74
MHCIIx (%)	6.5 (± 4.2)	5.0 (± 2.4)	0.46

$\dot{V}O_{2max}$: Maximal oxygen consumption. MHC: Myosin heavy chain. Values are mean (± 95% CI).

Table 2. Upregulated proteins in HIT (n = 9)

Name	Description	Log_2-change	q-value
GYS1	Glycogen [starch] synthase, muscle	0.46	≤ 0.01
FUNDC2	FUN14 domain-containing protein 2	0.91	≤ 0.05
NDUFA2	NADH dehydrogenase [ubiquinone] 1 alpha subcomplex subunit 2	0.38	≤ 0.05
COX6C	Cytochrome c oxidase subunit 6C	0.63	≤ 0.05
S100A13	Protein S100-A13	1.15	≤ 0.05
DNAJA2	DnaJ homolog subfamily A member 2	1.00	≤ 0.05
NDUFS6	NADH dehydrogenase [ubiquinone] iron-sulfur protein 6, mitochondrial	0.54	≤ 0.05
NDUFB6	NADH dehydrogenase [ubiquinone] 1 beta subcomplex subunit 6	0.51	≤ 0.05
UQCRH	Cytochrome b-c1 complex subunit 6, mitochondrial	0.36	≤ 0.05
MRPL12	39S ribosomal protein L12, mitochondrial	1.04	≤ 0.05
NDUFB3	NADH dehydrogenase [ubiquinone] 1 beta subcomplex subunit 3	0.40	≤ 0.05
PHB	Prohibitin	0.29	≤ 0.05
B2M	Beta-2-microglobulin;Beta-2-microglobulin form pI 5.3	0.97	≤ 0.05

ATP5H	ATP synthase subunit d, mitochondrial	0.28	≤ 0.05
SSBP1	Single-stranded DNA-binding protein, mitochondrial	0.22	≤ 0.05
MYOZ2	Myozenin-2	0.48	≤ 0.05
NDUFV2	NADH dehydrogenase [ubiquinone] flavoprotein 2, mitochondrial	0.28	≤ 0.05
STOML2	Stomatin-like protein 2, mitochondrial	0.43	≤ 0.05
ATP5J	ATP synthase-coupling factor 6, mitochondrial	0.35	≤ 0.05
COX5A	Cytochrome c oxidase subunit 5A, mitochondrial	0.24	≤ 0.05
PLIN2	Perilipin-2	0.39	≤ 0.05
NDUFB8	NADH dehydrogenase [ubiquinone] 1 beta subcomplex subunit 8, mitochondrial	0.55	≤ 0.05
SDHA	Succinate dehydrogenase [ubiquinone] flavoprotein subunit, mitochondrial	0.14	≤ 0.05
CHCHD3	Coiled-coil-helix-coiled-coil-helix domain-containing protein 3, mitochondrial	0.30	≤ 0.05
AGL	Glycogen debranching enzyme;4-alpha-glucanotransferase;Amylo-alpha-1,6-glucosidase	0.23	≤ 0.05
IMMT	Mitochondrial inner membrane protein	0.20	≤ 0.05

Table 3. Downregulated proteins in HIT (n = 9)

Name	Description	Log_2-change	q-value
PARK7	Protein DJ-1	-0.25	≤ 0.05
MYBPC1	Myosin-binding protein C, slow-type	-0.23	≤ 0.05
MYH1	Myosin-1	-0.48	≤ 0.05
PNPO	Pyridoxine-5-phosphate oxidase	-0.31	≤ 0.05
FKBP3	Peptidyl-prolyl cis-trans isomerase FKBP3	-0.25	≤ 0.05
HSPB1	Heat shock protein beta-1	-0.19	≤ 0.05

Table 4. Upregulated proteins in HIT+β_2A (n = 12)

Name	Description	Log_2-change	q-value
S100A13	Protein S100-A13	1.80	≤ 0.001
ACTG1	Actin, cytoplasmic 2;Actin, cytoplasmic 2, N-terminally processed	0.97	≤ 0.001
B2M	Beta-2-microglobulin;Beta-2-microglobulin form pI 5.3	1.22	≤ 0.01
PADI2	Protein-arginine deiminase type-2	0.41	≤ 0.01
SDHA	Succinate dehydrogenase [ubiquinone] flavoprotein subunit, mitochondrial	0.25	≤ 0.01
AHNAK	Neuroblast differentiation-associated protein AHNAK	0.44	≤ 0.01
PCBP1	Poly(rC)-binding protein 1	0.49	≤ 0.01
EEF1A1P5;EEF1A1	Putative elongation factor 1-alpha-like 3;Elongation factor 1-alpha 1	1.96	≤ 0.01
HK1	Hexokinase-1	0.47	≤ 0.01
YWHAZ	14-3-3 protein zeta/delta	0.27	≤ 0.01
ACSL1	Long-chain-fatty-acid--CoA ligase 1	0.35	≤ 0.01
PACSIN3	Protein kinase C and casein kinase substrate in neurons protein 3	0.24	≤ 0.01
S100A6	Protein S100-A6	0.68	≤ 0.01
DES	Desmin	0.39	≤ 0.05
ACTR3	Actin-related protein 3	0.40	≤ 0.05

RPL5	60S ribosomal protein L5	0.31	≤ 0.05
STOML2	Stomatin-like protein 2, mitochondrial	0.49	≤ 0.05
HSPA5	78 kDa glucose-regulated protein	0.30	≤ 0.05
MAPT	Microtubule-associated protein tau	0.40	≤ 0.05
ANP32A	Acidic leucine-rich nuclear phosphoprotein 32 family member A	1.58	≤ 0.05
RPSA	40S ribosomal protein SA	0.43	≤ 0.05
PDIA6	Protein disulfide-isomerase A6	0.59	≤ 0.05
HNRNPK	Heterogeneous nuclear ribonucleoprotein K	0.37	≤ 0.05
MYL9	Myosin regulatory light polypeptide 9	0.87	≤ 0.05
PPP1R14B	Protein phosphatase 1 regulatory subunit 14B	0.52	≤ 0.05
TOM1	Target of Myb protein 1	0.31	≤ 0.05
HADHA	Trifunctional enzyme subunit alpha, mitochondrial	0.32	≤ 0.05
NDUFC2	NADH dehydrogenase [ubiquinone] 1 subunit C2	0.73	≤ 0.05
TIMM50	Mitochondrial import inner membrane translocase subunit TIM50	0.69	≤ 0.05
NDUFS1	NADH-ubiquinone oxidoreductase 75 kDa subunit, mitochondrial	0.33	≤ 0.05
ACTC1	Actin, alpha cardiac muscle 1	1.21	≤ 0.05
PFN1	Profilin-1	0.25	≤ 0.05
MAOB	Amine oxidase [flavin-containing] B	0.59	≤ 0.05
MYL6	Myosin light polypeptide 6	0.96	≤ 0.05

Table 5. Downregulated proteins in HIT+β_2A (n = 12)

Name	**Description**	**Log_2-change**	**q-value**
HSPB1	Heat shock protein beta-1	-0.49	≤ 0.001
ALDH9A1	4-trimethylaminobutyraldehyde dehydrogenase	-0.25	≤ 0.001
GYG1	Glycogenin-1	-0.62	≤ 0.001
CFL2	Cofilin-2	-0.36	≤ 0.001
FHL1	Four and a half LIM domains protein 1	-0.31	≤ 0.001
PTGR2	Prostaglandin reductase 2	-0.36	≤ 0.001
CRYAB	Alpha-crystallin B chain	-0.30	≤ 0.01
HSPA2	Heat shock-related 70 kDa protein 2	-0.35	≤ 0.01
GSTM2	Glutathione S-transferase Mu 2	-0.30	≤ 0.01
ST13	Hsc70-interacting protein	-0.22	≤ 0.01
CMBL	Carboxymethylenebutenolidase homolog	-0.32	≤ 0.01
HSPB7	Heat shock protein beta-7	-0.33	≤ 0.01
DNPEP	Aspartyl aminopeptidase	-0.28	≤ 0.01
ACO1	Cytoplasmic aconitate hydratase	-0.25	≤ 0.01
AGL	Glycogen debranching enzyme	-0.32	≤ 0.01
MACROD1	O-acetyl-ADP-ribose deacetylase MACROD1	-0.20	≤ 0.01
PSMA6	Proteasome subunit alpha type-6	-0.23	≤ 0.01
PSMB3	Proteasome subunit beta type-3	-0.32	≤ 0.01
NDRG2	Protein NDRG2	-0.23	≤ 0.01
MDH1	Malate dehydrogenase, cytoplasmic	-0.23	≤ 0.01
CUTC	Copper homeostasis protein cutC homolog	-0.42	≤ 0.05
PDLIM5	PDZ and LIM domain protein 5	-0.23	≤ 0.05

CAB39	Calcium-binding protein 39	-0.26	≤ 0.05
NDUFB7	NADH dehydrogenase [ubiquinone] 1 beta subcomplex subunit 7	-0.54	≤ 0.05
PREP	Prolyl endopeptidase	-0.24	≤ 0.05
TPM3	Tropomyosin alpha-3 chain	-0.41	≤ 0.05
WDR1	WD repeat-containing protein 1	-0.18	≤ 0.05
LMCD1	LIM and cysteine-rich domains protein 1	-0.29	≤ 0.05
PSMA5	Proteasome subunit alpha type-5	-0.24	≤ 0.05
TNNC1	Troponin C, slow skeletal and cardiac muscles	-0.30	≤ 0.05
MAPRE2	Microtubule-associated protein RP/EB family member 2	-0.44	≤ 0.05
YWHAG	14-3-3 protein gamma;14-3-3 protein gamma, N-terminally processed	-0.20	≤ 0.05
TXLNB	Beta-taxilin	-0.24	≤ 0.05
PYGM	Glycogen phosphorylase, muscle form	-0.31	≤ 0.05
LDB3	LIM domain-binding protein 3	-0.17	≤ 0.05
TPM2	Tropomyosin beta chain	-0.44	≤ 0.05
AMPD1	AMP deaminase 1	-0.33	≤ 0.05
LMNB2	Lamin-B2	-0.84	≤ 0.05
ACADM	Medium-chain specific acyl-CoA dehydrogenase, mitochondrial	-0.27	≤ 0.05
PRDX1	Peroxiredoxin-1	-0.17	≤ 0.05
CRYZ	Quinone oxidoreductase	-0.26	≤ 0.05
TPT1	Translationally-controlled tumor protein	-0.17	≤ 0.05
PHPT1	14 kDa phosphohistidine phosphatase	-0.16	≤ 0.05
PFN2	Profilin-2	-0.99	≤ 0.05
MYOM2	Myomesin-2	-0.21	≤ 0.05
NPEPPS	Puromycin-sensitive aminopeptidase	-0.17	≤ 0.05
ATP2A2	Sarcoplasmic/endoplasmic reticulum calcium ATPase 2	-0.29	≤ 0.05
PCBD2	Pterin-4-alpha-carbinolamine dehydratase 2	-0.34	≤ 0.05
LDHA	L-lactate dehydrogenase A chain	-0.19	≤ 0.05
NT5C1A	Cytosolic 5-nucleotidase 1A	-0.46	≤ 0.05
PARK7	Protein DJ-1	-0.15	≤ 0.05

Table 6. Between-group interaction (HIT+β_2A – HIT)

Name	Description	Log_2-change	q-value
GYG1	Glycogenin-1	-0.67	≤ 0.01
HSPB7	Heat shock protein beta-7	-0.53	≤ 0.01
AGL	Glycogen debranching enzyme	-0.55	≤ 0.01
ACTG1	Actin, cytoplasmic 2;Actin, cytoplasmic 2, N-terminally processed	0.94	≤ 0.01
FHL1	Four and a half LIM domains protein 1	-0.31	≤ 0.01
CFL2	Cofilin-2	-0.31	≤ 0.01
GYS1	Glycogen [starch] synthase, muscle	-0.52	≤ 0.01
ATP2A2	Sarcoplasmic/endoplasmic reticulum calcium ATPase 2	-0.59	≤ 0.05
TNNC1	Troponin C, slow skeletal and cardiac muscles	-0.50	≤ 0.05
CRYAB	Alpha-crystallin B chain	-0.31	≤ 0.05
ALDH9A1	4-trimethylaminobutyraldehyde dehydrogenase	-0.17	≤ 0.05
ACO1	Cytoplasmic aconitate hydratase	-0.28	≤ 0.05
NDUFS6	NADH dehydrogenase [ubiquinone] iron-sulfur protein 6, mitochondrial	-0.68	≤ 0.05
TPM3	Tropomyosin alpha-3 chain	-0.62	≤ 0.05

PYGM	Glycogen phosphorylase, muscle form	-0.50	≤ 0.05
LDB3	LIM domain-binding protein 3	-0.26	≤ 0.05
MRPS36	28S ribosomal protein S36, mitochondrial	-0.44	≤ 0.05
PSMB3	Proteasome subunit beta type-3	-0.37	≤ 0.05
NDUFB6	NADH dehydrogenase [ubiquinone] 1 beta subcomplex subunit 6	-0.57	≤ 0.05
NDUFB7	NADH dehydrogenase [ubiquinone] 1 beta subcomplex subunit 7	-0.64	≤ 0.05
HSPB1	Heat shock protein beta-1	-0.29	≤ 0.05
HIST1H1C;HIST1H1E HIST1H1D	Histone H1.2;Histone H1.4;Histone H1.3	0.51	≤ 0.05
LMCD1	LIM and cysteine-rich domains protein 1	-0.39	≤ 0.05
SSBP1	Single-stranded DNA-binding protein, mitochondrial	-0.27	≤ 0.05
ACTN1	Alpha-actinin-1	0.61	≤ 0.05
AHNAK	Neuroblast differentiation-associated protein AHNAK	0.43	≤ 0.05
MRPL12	39S ribosomal protein L12, mitochondrial	-1.23	≤ 0.05
TPM2	Tropomyosin beta chain	-0.62	≤ 0.05
HK1	Hexokinase-1	0.44	≤ 0.05
YWHAZ	14-3-3 protein zeta/delta	0.28	≤ 0.05
NDUFA2	NADH dehydrogenase [ubiquinone] 1 alpha subcomplex subunit 2	-0.30	≤ 0.05
KPNB1	Importin subunit beta-1	0.71	≤ 0.05